CODEN:LUTEDX/(TEIE-5305)/1-58/(2012)

Industrial Electrical Engineering and Automation

Capacitive power transfer to car through wheel – is it possible?

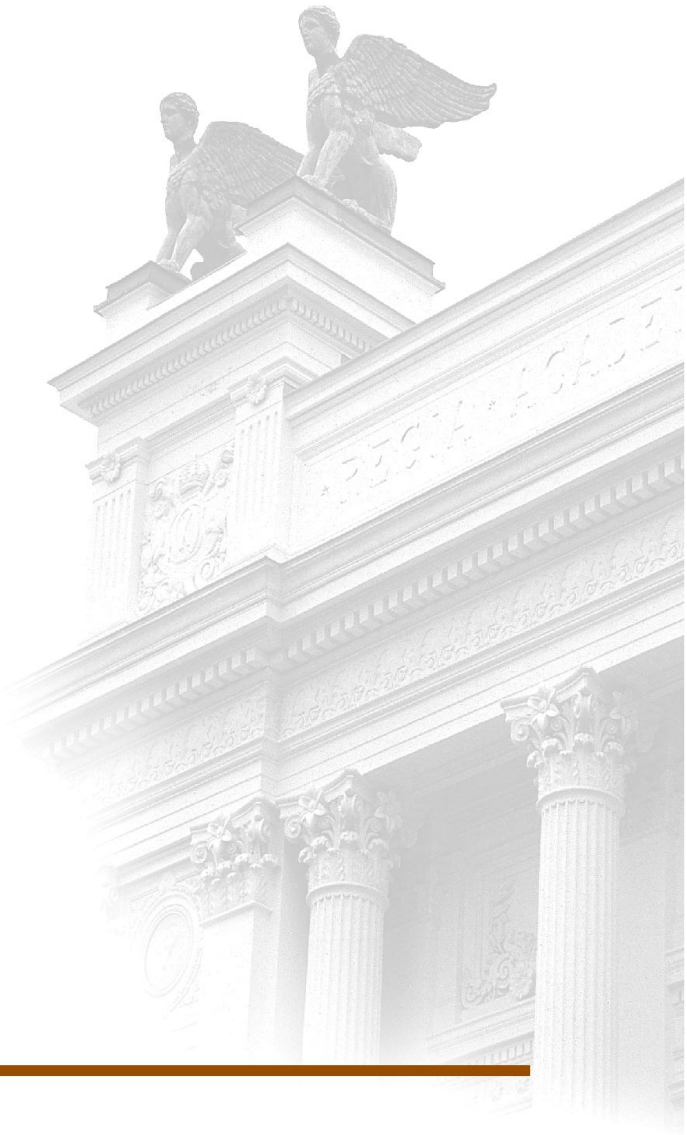

Sebastian Hall

Division of Industrial Electrical Engineering and Automation
Faculty of Engineering, Lund University

CAPACITIVE POWER TRANSFER TO CAR THROUGH WHEEL - IS IT POSSIBLE?

By

Sebastian Hall

Supervisors

Mats Alaküla, Avo Reinap

Division of Industrial Electrical Engineering and Automation
Faculty of Engineering, Lund University

September 2012

LUNDS UNIVERSITET
Lunds Tekniska Högskola

CONTENTS

LIST OF TABLES

LIST OF FIGURES

ACKNOWLEDGMENT

First and foremost I would like to thank Mats Alaküla, who made this project possible, and Avo Reinap, for all the time invested - Thank you!

I also would want to thank the whole IEA staff - with Getachew Darge, Fadi Abdallah and Lars Lindgren in the forefront - for good company and support, this work would have been a thousand times harder without you.

A special thanks goes out to the department for electrical measurements in LTH for letting me borrow their frequency analyzer, much appreciated.

Last but not least I would like to thank my cousins boyfriend Axel who helped me fetch the car tires that are used in this work, you are the man!

ABSTRACT

Introduction: This work aims to evaluate the possibility to transfer electrical power from a metal plate to the steel-cord within a car tire. If the tire stands on the plate, a connecting surface occurs which can be interpreted as a capacitor, where the rubber compound acts as a dielectric.

Method: First the impedance of the tire is evaluated: An analytical model is set-up to describe the system; a finite element simulation is made using the FEMM software and finally measurements using a Hewlett Packard 4194A impedance analyzer is made on a Dunlop SP Sport Maxx Tire.

Secondly, the possible power transfer is analyzed, both by creating an analytical model including the wheel impedance and a load, and by doing experiments on a real tire. The experiments and simulations are conducted both with and without a resonant inductor. LTspice models are made to support the practical results as far as possible and to investigate the limits for the capacitive power transfer.

Finally, a discussion is held regarding which parameters that can be improved to enhance the technique.

Results: The impedance measurements show that the impedance coupling has a capacitance of around 200 pF, and an equivalent series resistance which is inversely dependent on the frequency and has a value of 4400 Ω at a frequency of 10 kHz.

The LTspice simulations show that the imperfections in the transformer and the inductance that are used in the practical experiments give rise to a lot of losses. This makes the results from the analytical model and the practical experiments differ, especially when a resonant inductance is introduced.

For a square wave source voltage of 1600 V and 10 kHz, and a load of 50 kΩ, the analytical model give a load power of 20.1 W with an efficiency of 89 %. The practical experiments give a load power of 19.5 W with an efficiency of 81 % when a DC-link voltage of 30 V which results in a voltage about 1600 V on the secondary

side of the transformer - is used. For the same source voltage and load conditions, but with a resonant inductor introduced, the simulations give a load power of 34 W with an efficiency of 89 %. The practical experiments give a load power of 25 W with an efficiency of 76% (33 V out from the DC link).

Conclusion: This thesis shows that the impedance feature of the tire that is investigated makes it inappropriate for a big electrical power transfer. The capacitive element of the impedance can be compensated for with a resonant inductor, but the resistive part of the tire impedance is much too big to pass a lot of electrical energy. With a different rubber compound though, that would have a smaller dielectric loss angle, the technique could be worth evaluating more. For example, a tire with silica filler instead of carbon black filler - which is used in the tire of this project - could be worth analyzing.

1. INTRODUCTION

With the ongoing discussion about global warming due to CO_2 emissions and oil prices running high, an alternative to fossil-fuels in the transport-sector is becoming more and more relevant [1]. A number of solutions have been presented to make this come true: biofuels, with ethanol as the biggest alternative but with biogas and RME coming strong [1]; hydrogen fuel cells that drives an electrical motor through electrolysis; electrical hybrid cars with batteries as power sources etc. Electric cars seem to be a big factor in the transition from a fossil-fuel free vehicle fleet, but so far the limited driving range and the short lifetime of the battery have been limiting factors. These problems would be more or less eliminated with the possibility to charge the vehicle continuously while driving: the driving range would of course increase, and since the depth of discharge would decrease on the battery the lifetime would go up exponentially [2].

To be able to drive an electrical vehicle with power from the road, one would need to be able to extract several tens of kW:s. For example, a Nissan leaf has an electrical machine of 80 kW for a motor. Assuming that the long haulers also should be able to charge continuously, powers up to half a megaWatt could be used.

This study examines the possibilities to charge electrical cars from the ground through the tire with a capacitive power transfer. With metal on the ground, charged with an alternating voltage, power should hypothetically be able to transfer through the steel-cord in a car tire to a load. The purpose of this work then, is to evaluate if this technique is realistic seen from a technical point of view, and to determine which parameters that influence the power transfer the most. The workflow will be as follows:

The idea of the concept is firstly presented in more detail. The impedance of the capacitive coupling between the metal plate and the steel cord is investigated by first doing a finite element simulation of the system, and secondly by measuring the impedance on a real tire with a variable frequency impedance analyzer. Based

[1] For example, Sweden aims to have a vehicle fleet completely independent of fossil-fuels till 2030 [1]

on the derived impedance values, the power transfer is investigated theoretically by obtaining an analytical model of the system. A practical experiment is conducted to further analyze the system and to confirm the analytical models. Finally, a conclusion is drawn whether this technique is realistic for a future implementation or not.

2. THE IDEA

The idea for this project is to use the steel cord within a car tire to transfer electrical energy from metal plates in the ground to a car. The technique has been evaluated before [3], but this thesis aims to evaluate the concept more thoroughly, and the goal is to transfer power through a real car tire.

Figure 2.1 is showing a cross section of a tire (the model of the tire is the same that will be used in the practical experiments). As can be seen, a steel cord consisting of a steel thread that is wound several turns along the wearing surface is there for reinforcement. Supposing that the tire stands on a metal plate, there are two metal surfaces - the plate and the steel cord - that lies in parallel with each other. Considering the tire rubber to be a dielectricum, this can be interpreted as a capacitance, which means that an alternating electric field will pass energy from one surface (the plate) to another (the cord). This is the basic thought behind the modeling and the experiments that are to come.

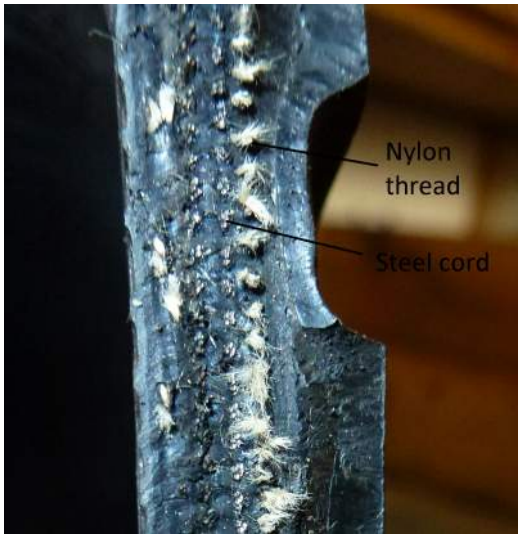

Figure 2.1: Cross section of a tire

Figure 2.2 is showing a basic sketch of the system. Since the system is considered symmetrical, only one capacitive coupling is taken into account for. The concept is to have a direct galvanic connection with the steel cord and to transfer

the power through the drive shaft directly to the power train (which is modelled as a load in Figure 2.2). Other techniques of using the capacitive coupling could be possible: The steel cord could be considered to be an intermediate conductor with an additional capacitve coupling to a conducting surface (for example aluminum foil) inside of the tire; the fender could be used as a conducting surface creating a capacitive coupling together with the cord in the top of the tire (this could eliminate possible problems with conducting electrical power through the drive shaft). The reason for chosing the technique with direct contact with the steel cord is to minimize the number of capacitive couplings in the system.

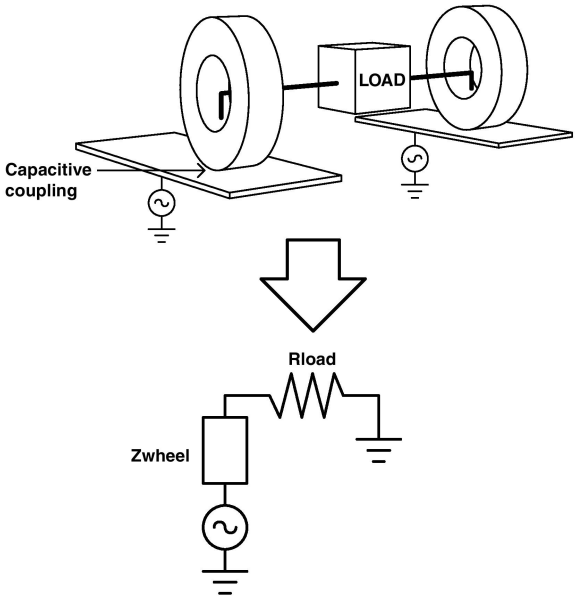

Figure 2.2: Model of system

3. IMPEDANCE OF TIRE

To be able to evaluate whether a capacitive power transfer through a car wheel is realistic or not, it is vital to have a perception of the impedance value of the tire . In this chapter, the tire impedance is investigated in the following order: An approximated analytical model for the impedance is formulated; simulations using the femm software is made; practical experiments on a real car tire is conducted; a sensitivity analysis is made and a the loss angle of the capacitive coupling is investigated.

3.1 Analytical model

An analytical model is set up to understand how the different parameters of the tire correlate with the impedance.

3.1.1 Capacitance

To do an accurate analytical model of the capacitance is hard because of the symmetry of the wheel. To get an idea of how the capacitance of the tire correlates with the different parameters though, it can be interesting to set up an equation which divides the capacitance into two parts: The capacitance due to the connecting surface of the wheel and the ground - approximated to be dependent only on the connection area, the depth of the rubber and the permittivity of the rubber - and the capacitance from the part of the wheel that is not connected to the ground - approximated to vary with the width of the tire and the permittivity of the rubber. The equation for the model is shown as equation 3.1, where ε is the relative permittivity of the rubber, A the connected area, d the depth of the rubber, w the width of the tire and k a constant.

$$C_{wheel} = \varepsilon_{rub}(\frac{A_{con}}{d} + kw) \tag{3.1}$$

A more detailed model of the capacitance is shown in equation 3.3. Here the part of the wheel that is not connected with the ground is approximated by a

number of equally big rectangles that is parallel with - and has different distance $\delta(i)$ from the ground. Since the capacitance of the rectangles has two dielectricum in series (the air and the rubber), the total capacitance has to be calculated adding the two resulting voltages together:

$$\begin{aligned} V_{tot} &= \frac{q}{C_{tot}} = V_{air} + V_{rub} = \frac{q}{C_{air}} + \frac{q}{C_{rub}} \rightarrow \\ C_{tot} &= \frac{1}{\frac{1}{C_{air}} + \frac{1}{C_{rub}}} = \frac{1}{(\frac{d}{\varepsilon_{rub} A_{rec}} + \frac{\delta(i)}{\varepsilon_{air} A_{rec}})} \end{aligned} \tag{3.2}$$

By making the rectangels smaller it is theoreticaly possible to achieve a accurate model of the total capacitive coupling.

$$C_{wheel} = \varepsilon_{rub} \frac{A_{con}}{d} + \sum_{i=1}^{n} \frac{1}{(\frac{d}{\varepsilon_{rub} A_{rec}} + \frac{\delta(i)}{\varepsilon_{air} A_{rec}})} \tag{3.3}$$

3.1.2 Dissipation factor and equivalent serie resistance

The dissipation factor (DF), or the tangent of the loss angle δ, is defined in equation 3.4 [9]. This factor specifies how big the resistive part of the impedance is in relation to the capacitive part. ε_r' is the relative permittivity of the rubber/air [2], ε_r'' is the relative loss factor of the rubber/air, ε_0 is the permittivity of free space, σ_0 is the resistivity of the rubber/air and ω is the angular frequency.

$$DF(\omega) = tan(\delta(\omega)) = \frac{\varepsilon_r''(\omega)}{\varepsilon_r'(\omega)} + \frac{\sigma_0}{\varepsilon_0 \varepsilon_r'(\omega)\omega} \tag{3.4}$$

The DF can be divided into two factors: The loss due to polarization, which is represented by the first part of equation 3.4, and the conductive losses, which is represented by the second part of equation 3.4. The equivalent series resistance (ESR) then - which represents the real part of the wheel impedance - is defined by multiplying the DF with the pure capacitive part of the wheel impedance (Equation 3.5).

[2]The dissipation factor for the part of the capacitance that is due to the connected surface between the tire and ground can be calculated by using the parameter values that are specified by the rubber. For the rest of the capacitance though, air will work as an dielectric as well, and the parameters are harder to specify

$$ESR(\omega) = \frac{DF(\omega)}{\omega C_{wheel}} \tag{3.5}$$

3.1.3 Complete impedance

The complete impedance of the tire is simply adding the capacitive and the resistive part together, creating a complex impedance (equation 3.6).

$$Z_{wheel}(\omega) = jX(\omega) + ESR(\omega) \tag{3.6}$$

3.2 Femm simulation

To get an idea of which value the capacitance of the wheel might have, a finite element simulation is made in the FEMM software. The model can be seen in Figure 3.1a and the result from the simulation can be seen in Figure 3.1b.

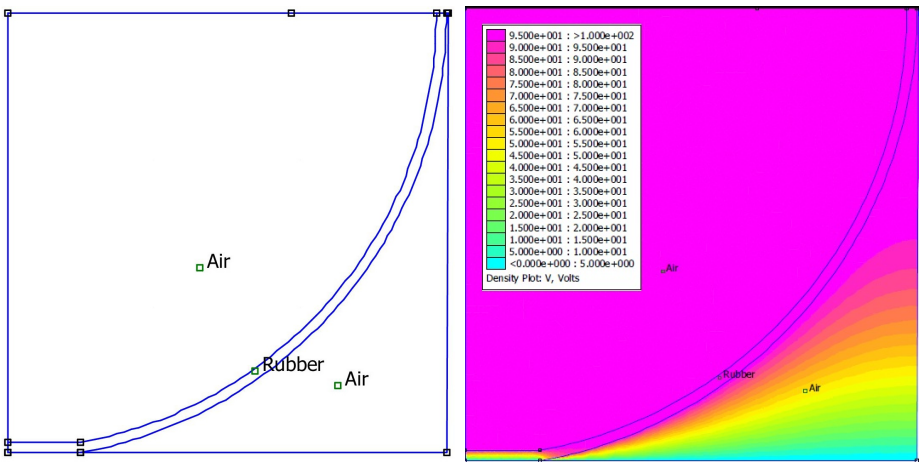

(a) femm simulation model (b) femm simulation results

Figure 3.1: Finite element simulation

Only a quarter of the wheel is modelled, and the capacitance value between the cord and the ground that is calculated must therefore be multiplied by two. The model is set to be 21 cm deep which is consistent with the dimensions of the tire used in the practical experiments. The outer radius of the model is 30 cm and the thickness of the rubber is considered to be 0.7 cm. The lateral length of the contact surface between the wheel and the ground is considered to be 10

cm, which is consistent with when the wheel used in the practical experiments stand on ground without pressure. The materials in the model are defined by their relative permittivity. In this case, the rubber is considered to have $\varepsilon' = 15$, which is consistent with a Styrene Butadiene Rubber (SBR) with 40 phr[3] carbon black (HAF) added [4]. The capacitance is calculated by applying a voltage - 100 V - from the line over the rubber to the lower line of the model. Figure 3.1b shows how the voltage distributes in the model when the simulation is made. By integrating the area in between the steel-cord and the ground, the program calculates the total stored energy within this area and the capacitance can be calculated with equation 3.7 [10].

$$C = \frac{2 \cdot W_{stored}}{V_{applyed}^2} \tag{3.7}$$

The simulation gives the capacitance $C_{wheel} = 238pF$.

3.2.1 Sensitivity analysis of capacitance value

The purpose of the sensitivity analysis is to examine how the different parameters of the tire affect the capacitive coupling. Geometry, as in contact surface with the ground and width of the tire, and the permittivity of the rubber will be varied. The results from the sensitivity analysis can be seen in Table 3.1.

As expected, the width and the permittivity have a linear relationship, whereas the depth has an inverse relationship with the capacitive coupling. The length of the connecting surface does not have an as linear relationship with the capacitive coupling (even though it is pretty close) since the capacitance which is not related to the connecting surface is changed as well (the bigger the surface, the lesser influence). The first term of (3.1) seems to be a pretty good approximation for the connected surface relationship to the wheel capacitance then, accepting the small fault in the length of the connecting surface.

The capacitance due to the part of the tire that is not connected to ground should be linearly dependent of the width of the tire and the permittivity of the

[3]Parts per hundred of rubber

CAPACITANCE					
Width (axial dimension in the FEMM model)	15 cm	20 cm	25 cm	30 cm	35 cm
CONNECTING SURFACE (lateral length of the connecting surface between the lower horizontal line and the outer diameter in the FEMM model) $\varepsilon = 15$, rubber depth = 7 mm, radius = 30 cm					
Surface = 0 cm	66.1 pF	88.1 pF	110 pF	132 pF	154 pF
Surface = 5 cm	109 pF	145 pF	181 pF	218 pF	254 pF
Surface = 10 cm	170 pF	226 pF	283 pF	340 pF	396 pF
Surface = 15 cm	236 pF	314 pF	393 pF	471 pF	550 pF
PERMITTIVITY = ε connecting surface = 10 cm, rubber depth = 7 mm, radius = 30 cm					
$\varepsilon = 1$	20.0 pF	26.6 pF	33.3 pF	40.0 pF	46.7 pF
$\varepsilon = 8$	98.0 pF	131 pF	163 pF	196 pF	229 pF
$\varepsilon = 15$	170 pF	226 pF	283 pF	340 pF	396 pF
$\varepsilon = 22$	241 pF	321 pF	401 pF	481 pF	562 pF
DEPTH (distance between the outer diameter to the cord diameter in the FEMM model) $\varepsilon = 15$, connecting surface = 10 cm, radius = 30 cm					
Depth = 4 mm	279 pF	373 pF	466 pF	559 pF	653 pF
Depth = 7 mm	170 pF	226 pF	283 pF	340 pF	396 pF
Depth = 10 mm	124 pF	167 pF	208 pF	250 pF	292 pF
Depth = 13 mm	100 pF	134 pF	167 pF	201 pF	234 pF

Table 3.1: Sensitivity analysis for tire capacitance

rubber if (3.1) is to be correct. Row 4 in Table 3.1 confirms a linear relationship between the capacitance and the width of the tire when the connecting surface is zero[4].

The rubbers permittivity relationship to the capacitance when the connecting surface is zero is investigated in Figure 3.2. Here it comes clear that the approximation that the capacitance is linear with the permittivity value of the rubber is not accurate at all, which makes the second term of (3.1) questionable. It should be mentioned tough that the total capacitance of the system only is marginally affected by this phenomenon when the connected surface has the length 10 cm (Figure 3.2)

[4]This is of course a theoretical scenario. In real life there has to be a connected surface if the tire stands on the ground.

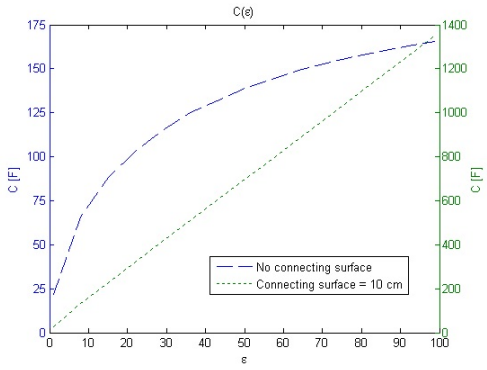

Figure 3.2: Capacitance as a function of ε

3.3 Measurements

The impedance of the connection between a steel plate and the steel-cord in the tire is measured with a Hewlett packard 4194A impedance/gain-phase analyzer. A plate of steel is set under the wheel and screws are screwed through the tire to assure galvanic connection with the steel cord. The set-up for the measurements can be seen in figure 3.3. Three measurements are made: The first one only putting the wheel on top of the metal plate, the second one with a pressure applied on top of the wheel and the third one with the inside of the tire coated in aluminum foil. The experiment when pressure is applied is conducted to see how a bigger contact area between the tire and the plate affects the impedance coupling. The experiment with the inside of the tire coated with aluminum foil is made to see if the capacitive coupling can be improved adding an additional connecting surface to the coupling.

3.3.1 Compensation for cabels

To compensate for the distortion that the cables give rise to, a test capacitance of 200 pF is used. Firstly, the impedance value of the capacitor is measured with a probe that is supposed to give nearly zero distortion. Secondly, the capacitor is measured with the measurement cables attached to it. The difference between the two measurements will be subtracted from the measurements on the capacitive coupling of the tire. This is by no means a perfect way to take account for the cables, but it will at least reduce the distortion. The result of the compensation

(a) Measurement without foil (b) Measurement with foil

Figure 3.3: Impedance mesurement set-ups

measurements can be seen in figure 3.4.

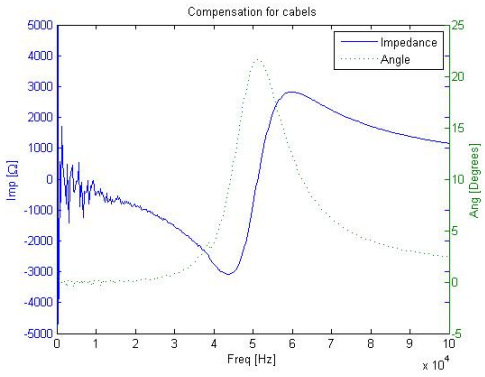

Figure 3.4: Compensation for cabels

3.3.2 Results

The results of the measurements without any pressure, with pressure and with aluminum foil can be seen in figure 3.5, figure 3.6a and figure 3.6b respectively. As can be seen, the capacitance value of the coupling rises with pressure but stays more or less the same with aluminum added to the system. The reason for the rise when pressure is added is due to the fact that the connecting surface between the tire and the metal plate is becoming bigger.

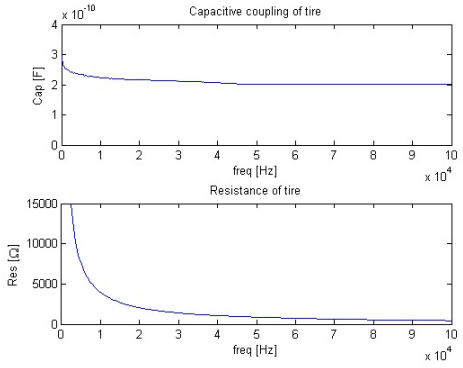

Figure 3.5: Impedance measurment of tire

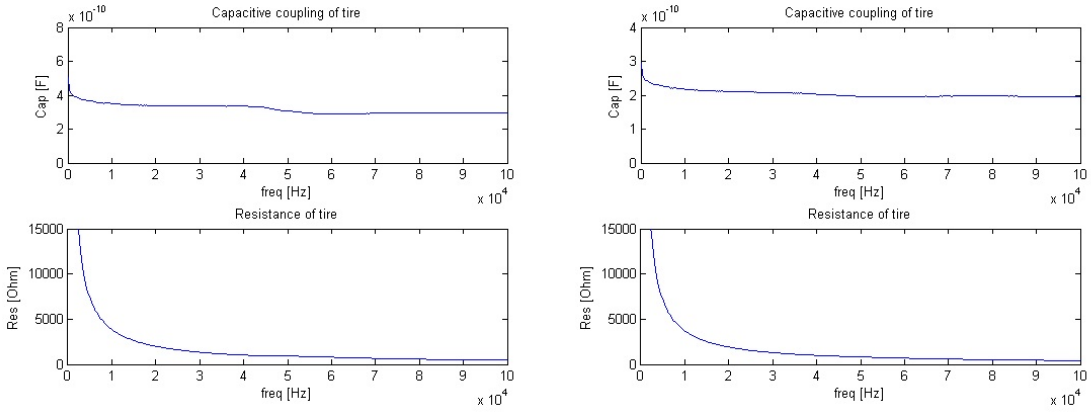

(a) Measurement with pressure (b) Measurement with aluminum

Figure 3.6: Impedance measurements

3.3.3 Loss angle

The dielectric loss angle of the rubber compound is a key factor for the possibility to tranfer power to the load from the source. Since the loss angle defines how big the resistive part of the tire impedance will be, it also determines how big the losses is. Supposing that resonant filter is used to compensate for the capacitance of the impedance coupling, the resistive part is the only thing that limits the current - hence the power transfer - through the tire.

Figure 3.7 is showing the tangent of the loss angel (the dissipation factor) as a function of frequency for the measurement without pressure. The oscillation around 50 kHz is due to the distortion that the measurements cables give rising to. As can be seen, the loss angle is decreasing with frequency at the beginning and starts to

increase with frequency again around 60 kHz. Since the angle does not obviously correlate with the inverse of the frequency, the losses are probably mostly due to polarization.

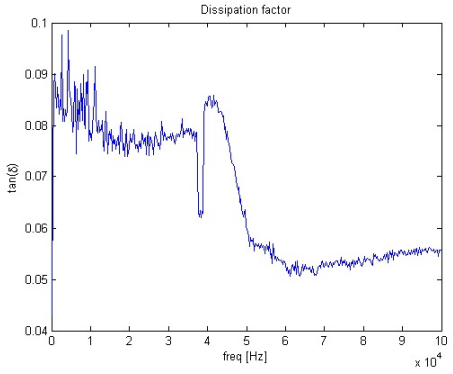

Figure 3.7: Dissipation factor

The values for the permittivity and the loss factor for Styrene Butadiene Rubber (SBR) with 40 phr carbon black (HAF) added [4], are $\varepsilon_r' = 15$ and $\varepsilon_r'' = 1.1$ when the frequency is equal to 10 kHz, which means that $DF = \frac{1.1}{15} = 0.073$, supposing that the conductive losses are negligible.

4. ANALYTICAL MODELS OF POWER TRANSFER

This chapter aims to describe the current, power and efficiency mathematically when a periodic voltage is applied to an equivalent circuit of the system os interest: First, a basic model consisting only of a source voltage, the wheel and a load resistor is considered; secondly, a series inductor - working as a resonant filter - is added to the system.

The systems is analyzed considering both a sinusoidal and a square wave source voltage. Both cases are interesting since a square wave voltage will be used in the practical experiments, but a close to sinusoidal voltage would probably be used in a real life implementation. The source voltage is considered to have a RMS value of 1608 V, which is the value that is used in the practical experiments. It should be mentioned that the power transfer and the losses have a quadratic correlation with the source voltage, and that the power transfer for a higher source voltage therefore easily can be derived from the results that is presented in this chapter. The impedance values that are used are the ones that were measured in the previous chapter.

Previous recent works that have investigated *inductive* power transfer to a car ([5]-[8]) have considered frequencies from 10 kHz to 38.4 kHz on the source voltage. Here, a frequency span of 0 - 100 kHz will be investigated to see how the frequency affects the power transfer. A special emphasis will be given to the case when the frequency is equal to 9.75 kHz since this is the frequency that will be used in the practical experiments.

4.1 Basic model

The first model aims to simulate the impedance coupling of the tire together with a load resistance. The assumed equivalent circuit is shown in Figure 4.1.

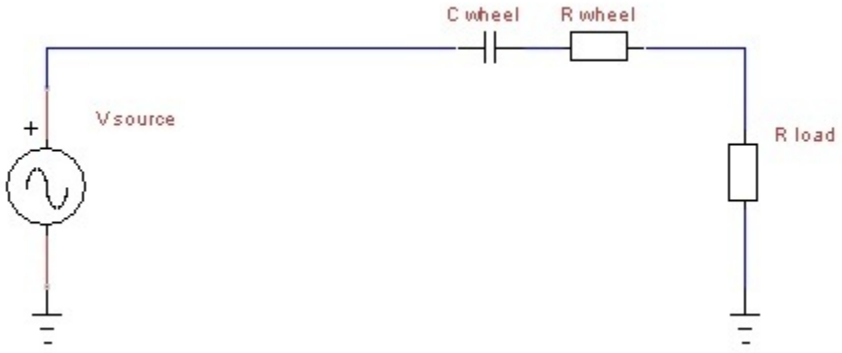

Figure 4.1: Basic RC-circuit which simulates the car tire in series with a load and a voltage source.

4.1.1 Sinusoidal voltage

Considering a sinusoidal source voltage and a steady-state situation, equations to derive the power is set up using phasors [10].

$$X_{wheel} = \frac{1}{w \cdot C_{wheel}} \tag{4.1}$$

$$I = \frac{V_{source}}{-j \cdot X_{wheel} + R_{wheel} + R_{load}} \tag{4.2}$$

$$P_{load} = R_{load} \cdot |I|^2 \tag{4.3}$$

A matlab script is written to simulate the power transfer as a function of the frequency and the load resistance, using (4.1), (4.2) and (4.3). The results from the impedance measurement is used for the parameters C_{wheel} and R_{wheel} (Figure 4.1). The result of the power over the load resistance is presented in Figure 4.2.

The losses in the wheel is calculated by multiplying the wheel resistance with the load current - which is the same current that will flow in the wheel resistance - powered by two (4.4). The efficiency (η) is calculated by dividing the load power with the load power plus the loss power (4.5). The losses and the efficiency plotted as function of load resistance and frequency can be seen in Figure 4.3 and Figure 4.4. Note the small oscillation around 50 kHz in the loss power when the load is small. This is due to the distortion of the cables used in the impedance measurements.

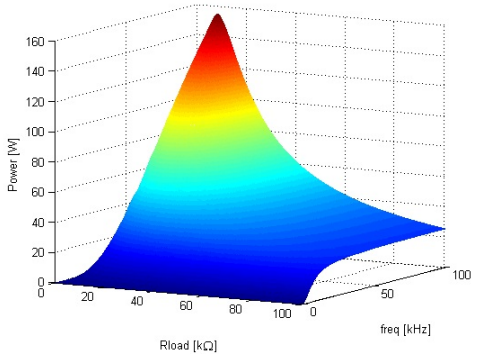

Figure 4.2: Load power with a sinusoidal source voltage as a function of load resistance and frequency.

$$P_{loss} = R_{wheel} \cdot |I|^2 \tag{4.4}$$

$$\eta = \frac{P_{load}}{P_{load} + P_{wheel}} \tag{4.5}$$

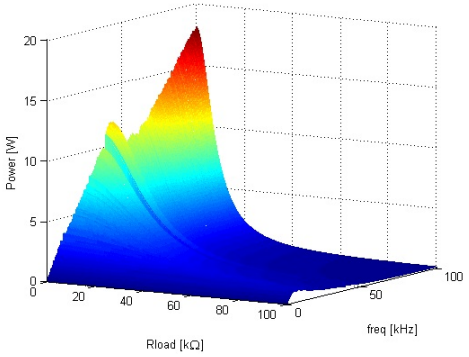

Figure 4.3: Power dissipated in the tire resistance with a sinusoidal source voltage as a function of load resistance and frequency.

Figure 4.5 is showing the transferred power as a function of the load resistance together with the losses and the efficiency, when the frequency is equal to 10 kHz. Since the load resistance has a very high value compared to the wheel resistance for any considerable power transfer, the loss power is very small compared to the load

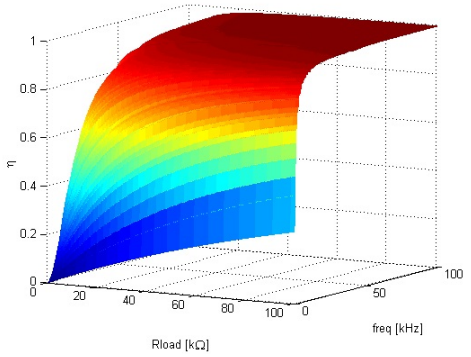

Figure 4.4: Efficiency with a sinusoidal source voltage as a function of load resistance and frequency.

power, and the efficiency is high.

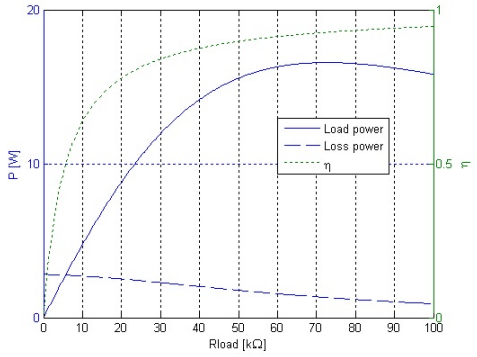

Figure 4.5: Load Power, loss power and efficiency with a sinusoidal source voltage with a frequency of 10 kHz, as a function of load resistance.

4.1.2 Squarewave voltage

A general mathematical expression for the system in time domain is set up [10].

$$u(t) = \frac{1}{C_{wheel}} \int i(t)dt + i(t)(R_{wheel} + R_{load}) \tag{4.6}$$

Using the laplace transform, an expression for the current in frequency domain can be deduced.

$$\mathcal{L}\{u(t)\} = \frac{i(s)}{s \cdot C_{wheel}} + (R_{wheel} + R_{load})i(s) \tag{4.7}$$

$$i(s) \quad = \quad i(t) = \frac{u(s)}{\frac{1}{s \cdot C_{wheel}} + R_{wheel} + R_{load}} \tag{4.8}$$

The current is expressed when considering the voltage to be a step [5].

$$u(s) \quad = \quad \frac{U}{s} \tag{4.9}$$

$$\begin{aligned} i(s) &= \frac{U}{\frac{1}{C_{wheel}} + s(R_{wheel} + R_{load})} \\ &= \frac{U}{R_{wheel} + R_{load}} \cdot \frac{1}{\frac{1}{C_{wheel}(R_{wheel}+R_{load})} + s} \end{aligned} \tag{4.10}$$

The parameters *time constant* $= \tau$ and the *amplitude* $= I_0$ are introduced (4.15, 4.16):

$$\tau \quad = \quad C_{wheel}(R_{wheel} + R_{load}) \tag{4.11}$$

$$I_0 \quad = \quad \frac{U}{R_{wheel} + R_{load}} \tag{4.12}$$

The expression for the current is brought back to time domain using inverse laplace transform.

$$\mathcal{L}^{-1}\{i(s)\} = I_0 e^{-\frac{t}{\tau}} \tag{4.13}$$

To derive an expression for the load power, the current that is flowing in the circuit is powered by two and multiplied with the load resistance.

$$p(t) = R_{load}|i(t)|^2 = R_{load}(I_0 e^{-\frac{t}{\tau}})^2 \tag{4.14}$$

$$\tau \quad = \quad C_{wheel}(R_{wheel} + R_{load}) \tag{4.15}$$

$$I_0 \quad = \quad \frac{U}{R_{wheel} + R_{load}} \tag{4.16}$$

The avarege power over the load is calculated by integrating one period of the power and dividing it by the time length of the period (4.17). T is considered to be the time of one current period - since the current is powered by two when calculating the power, the load power will have the double frequency, and the integration can

[5] This approximation is valid due to the fact that no transient will be apparent when the circuit is connected to the supply voltage. The second half period of the current will therefore be the same as the first - only with a different sign - and the current reaches a steady state situation directly.

be made from t=0 to t=T/2.

$$\begin{aligned} \bar{p} &= R_{load} I_0^2 \cdot \frac{2}{T} \int_0^{\frac{T}{2}} e^{\frac{-2t}{\tau}} dt \\ &= R_{load} I_0^2 \frac{-\tau}{2T} (e^{-\frac{T}{\tau}} - 1) \end{aligned} \tag{4.17}$$

The average power transfered to the load resistance as a function of frequency (1/T), and load resistance can be seen in Figure 4.6. The voltage is considered to have an RMS value of 1608 V.

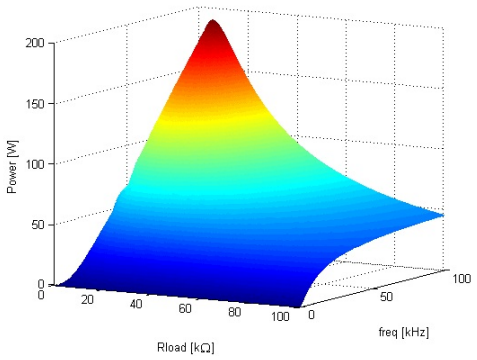

Figure 4.6: Load power with a squarewave source voltage as a function of load resistance and frequency.

The loss power (Figure 4.7) and the efficiency (Figure 4.8) are plotted as functions of frequency and load resistance using (4.4) and (4.5). The reader will notice the big difference in losses compared to when a sinusiodal voltage is used (Figure 4.3). This is due to the harmonics that are introduced with the square wave: All harmonics except the fundamental has a higher frequency than the square wave, hence the impedance of the capacitive coupling - which is inversely related to the frequency (4.1) - will go down. This means that for the harmonics with high frequency, the impedance due to the capacitor is much lower than the impedance from the wheel resistance. If the load resistance is close to zero then, the current will almost only be limited by the wheel resistance, and the losses will be high. This phenomena can be seen comparing Figure 4.2 with Figure 4.6 as well, as the Load power is bigger when a square wave is used than for when the sinusoidal voltage is applied.

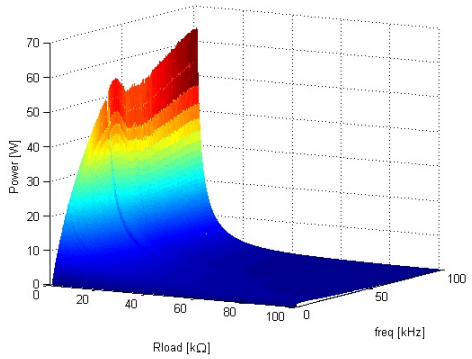

Figure 4.7: Power dissipated in the wheel resistance with a square wave source voltage as a function of load resistance and frequency.

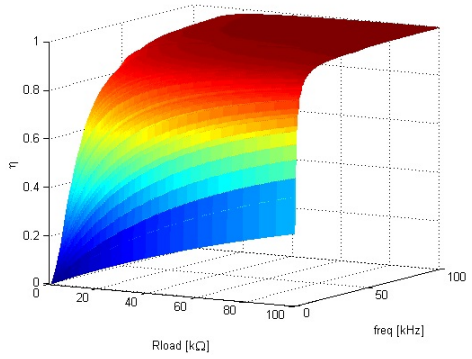

Figure 4.8: Efficiency with a square wave source voltage as a function of load resistance and frequency.

Figure 4.9 is showing the average power over the load resistance, the loss power and the efficiency at 10000 Hz frequency. Notice that the loss power - specially for lower values of the load resistance - is higher than if a sinusoidal voltage is used (Figure 4.5)

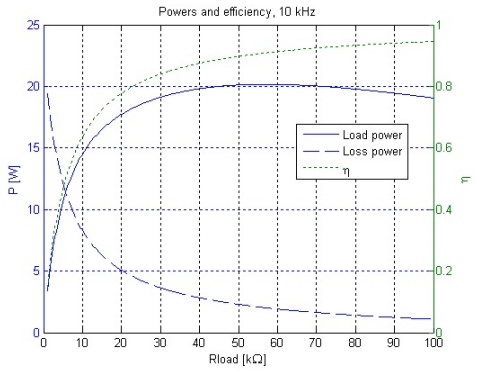

Figure 4.9: Load power, loss power and efficiency with a square wave source voltage with a 10 kHz frequency, as a function of load resistance.

4.2 Introducing a series inductance

To introduce a series inductance is interesting, partly because the transformer that will be used in the practical experiments will have a small leakage inductance, but foremost because the inductance can work as a resonance circuit. The equivalent circuit of the system can be seen in figure 4.10.

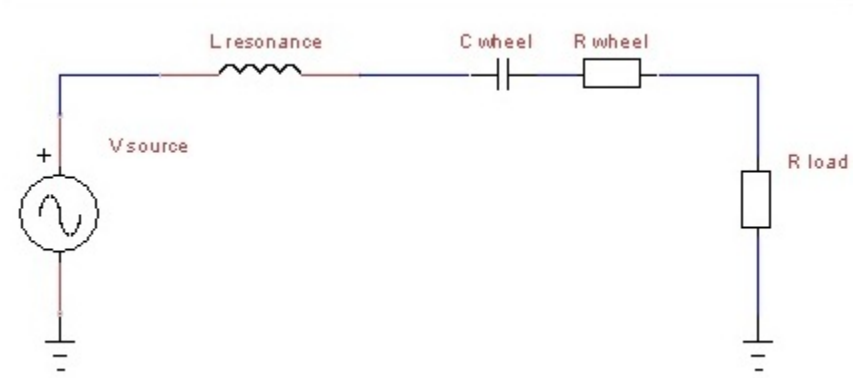

Figure 4.10: RCL equivalent circuit, simulating the wheel in series with a load resistance, the source voltage and a resonance inductance.

4.2.1 Sinusiodal voltage

Considering a sinusoidal source voltage and a steady-state situation, equations to derive the power is set up using phasors [10].

$$X_{wheel} = \frac{1}{w \cdot C_{wheel}} \tag{4.18}$$

$$X_{resonance} = w \cdot L_{resonance} \tag{4.19}$$

$$I = \frac{V_{source}}{j(L_{resonance} - X_{wheel}) + R_{wheel} + R_{load}} \tag{4.20}$$

$$P_{Rload} = R_{load} \cdot |I|^2 \tag{4.21}$$

If the inductor is to work as a resonance filter, the impedance from the inductor should be equal to the impedance from the capacitor, and the value of the inductance should be calculated as in (4.22).

$$L_{resonance} = \frac{1}{w^2 C_{wheel}} \tag{4.22}$$

A matlab script is written to simulate the power transfer as a function of the frequency and the load resistance, using (4.18), (4.19), (4.20) and (4.21). The value for $L_{resonance}$ is recalculated for each frequency according to 4.22. The results from the simulation can be seen in Figure 4.11. The results from the impedance measurement is used for the C_{wheel} and R_{wheel} parameters. As can be seen, since the imaginary part of equation 4.20 is 0, the current, hence the power, is only limited by the resistive part of the circuit. Since the wheel resistance vary much with the frequency of the voltage, so will the transferred power. A smaller wheel resistance gives a higher possible current, and a higher possible power transfer.

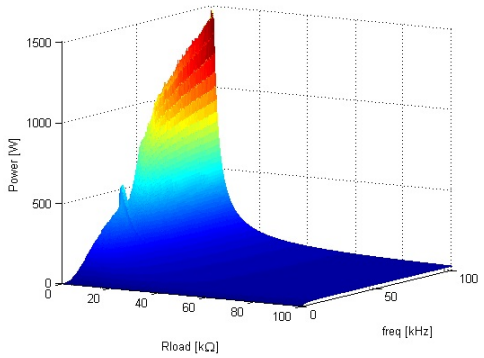

Figure 4.11: Load Power with a sinusoidal source voltage and a series inductance, as a function of load resistance and frequency.

The power losses and the efficiency are plotted in Figure 4.12 and Figure 4.13. Since the load resistance is lower than for the simulation without a series inductance, the losses in the wheel resistance will be bigger and the efficiency will be worse.

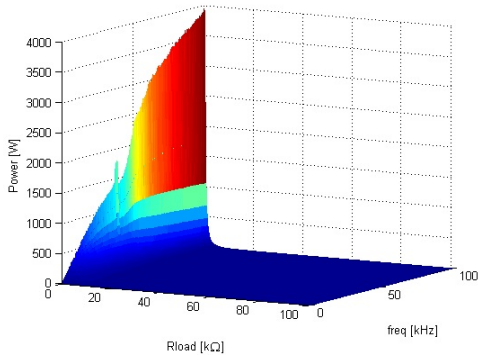

Figure 4.12: Power dissipated in the wheel resistance with a sinusoidal source voltage and a series inductance, as a function of load resistance and frequency.

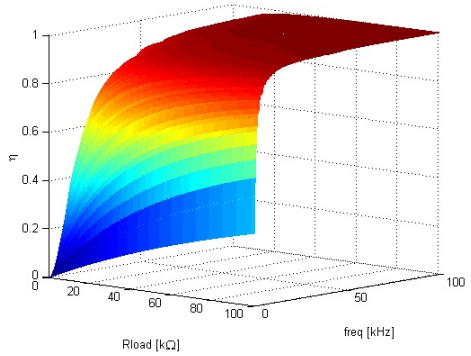

Figure 4.13: Efficiency with a sinusoidal source voltage with a resonance inductance, as a function of load resistance and frequency.

The power when the frequency is equal to 10 kHz can be seen in Figure 4.14. As can be seen the efficiency is 0.5 when the maximum load power is achieved, which means that the load resistance and the wheel resistance are equally big.

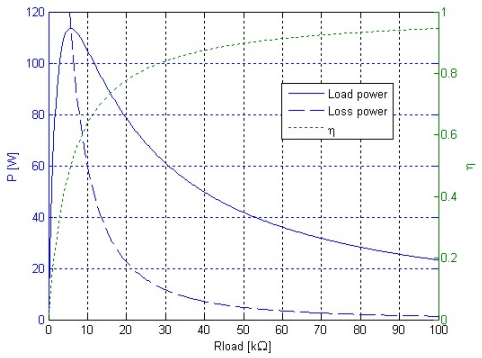

Figure 4.14: Load power, loss power and efficiency with a square wave source voltage with a 10 kHz frequency, as a function of load resistance.

4.2.2 Square wave voltage

A general mathematical expression for the circuit (Figure 4.10) in time domain is set up [10].

$$u(t) = L_{resonance}\frac{di}{dt} + \frac{1}{C_{wheel}}\int i(t)dt + i(t)(R_{wheel} + R_{load}) \tag{4.23}$$

An expression for the current in frequency domain is deduced using laplace transform.

$$\mathcal{L}\{u(t)\} = s \cdot L_{resonance}i(s) + \frac{i(s)}{s \cdot C_{wheel}} + (R_{wheel} + R_{load})i(s) \tag{4.24}$$

$$i(s) = \frac{u(s)}{s \cdot L_{resonance} + \frac{1}{s \cdot C_{wheel}} + R_{wheel} + R_{load}} \tag{4.25}$$

The voltage can no longer be approximated by a single step, since a large inductor introduces a transient not equal to steady state. Considering the voltage to be a sum of steps, with T as the time of one voltage period, the voltage and the current are expressed in frequency domain.

$$u(s) = \frac{U}{s}\sum_{i=0}^{n}(-1)^i e^{\frac{-iTs}{2}} \tag{4.26}$$

$$i(s) = \frac{U}{s^2 L_{resonance} + \frac{1}{C_{wheel}} + s(R_{wheel} + R_{load})}\sum_{i=0}^{n}(-1)^i e^{\frac{-iTs}{2}} \tag{4.27}$$

The $neperfrequency = \alpha$ and the $resonancefrequency = \omega_0$ are introduced.

$$\alpha = \frac{R_{load} + R_{wheel}}{2L_{resonance}} \tag{4.28}$$

$$\omega_0 = \frac{1}{\sqrt{LC}} \tag{4.29}$$

The heaviside step function is defined.

$$\theta(t-\tau) = \begin{cases} 0, & t-\tau < 0; \\ 1, & t-\tau \geq 0; \end{cases}$$

The equation for the current is brought back to time domain using inverse

laplace transform.

$$\mathcal{L}^{-1}\{i(s)\} = \frac{U}{2L\sqrt{\alpha^2-\omega_0^2}}\sum_{i=0}^{n}(-1)^i\theta(t-i\frac{T}{2})(e^{-(t-i\frac{T}{2})\cdot(\sqrt{\alpha^2-\omega_0^2}+\alpha)}-e^{-(t-i\frac{T}{2})\cdot(-\sqrt{\alpha^2-\omega_0^2}+\alpha)}) \tag{4.30}$$

The parameters *time constant 1* $= \tau_1$, *time constant 2* $= \tau_2$ and the *amplitude* $= I_0$ are introduced to make the expression shorter.

$$\tau_1 = \frac{1}{\sqrt{\alpha^2-\omega_0^2}+\alpha} \tag{4.31}$$

$$\tau_2 = \frac{1}{-\sqrt{\alpha^2-\omega_0^2}+\alpha} \tag{4.32}$$

$$I_0 = \frac{U}{2L\sqrt{\alpha^2-\omega_0^2}} \tag{4.33}$$

To calculate the average power over the load resistance, the method is similar to the one used in equation 4.14. This time though, the integration has to be made after signal has reached steady state. Considering that this is reached before period n, the average power is expressed in (4.34).

$$\bar{p} = R_{load}I_0^2\cdot\frac{2}{T}\int_{\frac{T}{2}(n-1)}^{\frac{T}{2}n}\sum_{i=0}^{n}(-1)^i\theta(t-i\frac{T}{2})(e^{\frac{-(t-i\frac{T}{2})}{\tau_1}}-e^{\frac{-(t-i\frac{T}{2})}{\tau_2}})dt \tag{4.34}$$

(4.34) is solved numerically in matlab and plotted as a function of $L_{resonance}$ and R_{load} (Figure 4.15). As expected the plot looks simular to Figure 4.11: The inductor filters all the harmonics except the fundamental away, which results in a sinusoidal load voltage. The power is smaller than when a sinusoidal voltage is used since the amplitude of the fundamental in the square wave ($\frac{4}{\pi}\cdot u_{sq-rms}$) is smaller than the amplitude of the sinusoidal voltage ($\sqrt{2}\cdot u_{sin-rms}$).

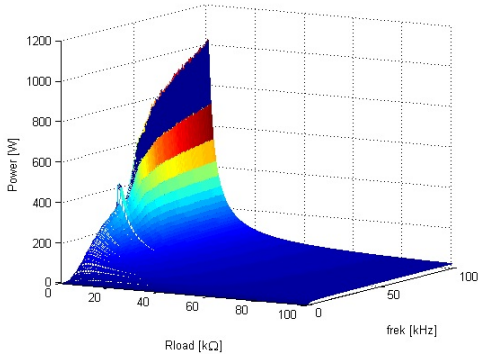

Figure 4.15: Load Power with a square wave source voltage and a series inductance, as a function of load resistance and frequency.

The loss power and the efficiency are plotted in Figure 4.16 and Figure 4.17, respectively. The results are very similar to the results when a sinusoidal voltage is used (Figure 4.12, Figure 4.13). Figure 4.18 is showing the load power, loss power and efficiency when the frequency of the source voltage is 10 kHz.

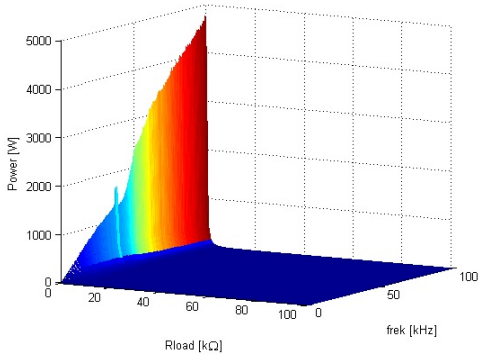

Figure 4.16: Power dissipated in the wheel resistance with a sinusoidal source voltage and a series inductance, as a function of load resistance and frequency.

4.2.3 Voltage between the dynamic elements

To have an idea about the voltage in between the dynamic elements is important, partly because a high voltage can give rise to big losses, but foremost because of safety issues. If the inductor is designed to resonate with the capacitor, the only thing that limit the current in the circuit is the resistive part, and the voltage over

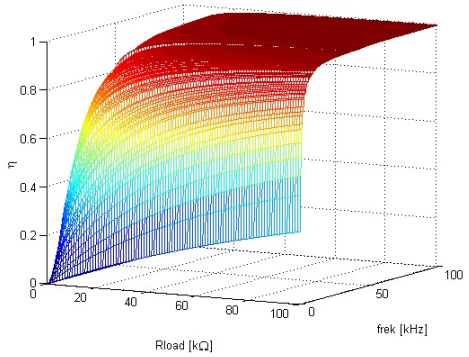

Figure 4.17: Efficiency with a square wave source voltage with a resonance inductance, as a function of load resistance and frequency.

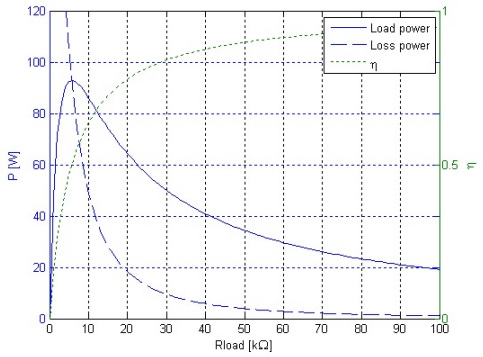

Figure 4.18: Load power, loss power and efficiency with a square wave source voltage with a 10 kHz frequency, as a function of load resistance.

the dynamic elements is formulated as in (4.36) and (4.37) [10]. X_{wheel} and $X_{resonance}$ are defined in (4.18) and (4.19).

$$i = \frac{u_{rms}}{R} \tag{4.35}$$

$$u_{cap} = \frac{i}{-jX_{wheel}} \tag{4.36}$$

$$u_{res} = \frac{i}{jX_{resonance}} \tag{4.37}$$

As can be understood from foregoing equations, big dynamic element impedances result in high voltages. With a low frequency the impedances become high and the

voltage goes up; with a low load resistance, the current flowing through the system becomes big, and the voltage goes up. Since X_{wheel} and $X_{resonance}$ are equally big and phase shifted 180 degrees, the voltage will go up passing the first dynamic element and come back down again passing the second. The voltage plotted as a function of load resistance and frequency can be seen in Figure 4.19.

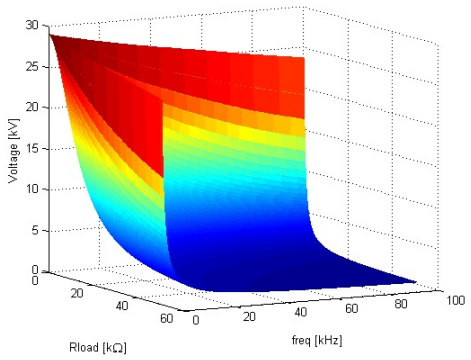

Figure 4.19: Voltage in between the dynamic elements plotted as a function of load resistance and frequency.

5. PRACTICAL EXPERIMENT

This chapter will explain how the practical experiments are conducted and present results from different measurement points.

5.1 Without resonant inductor

The first experiment is set up to mimic the first analytical model as far as possible, investigating how accurate the model is and where the imperfections will show.

5.1.1 The setup

The setup for the experiment is illustrated in Figure 5.1a and can be seen in Figure 5.1b. The experiments are driven by a four quadrant power inverter. The transistors of the inverter are controlled by a CompactRIO field-programmable gate array (fpga) that is programmed using the LabView software. Different values for the DC link voltage are supplied by a HQ power 3010 voltage source.

A transformer is introduced to the system to be able to achieve desirable voltage levels. The transformer has a ratio of 1:53.7 meaning that it will magnify the primary voltage 53.7 times. Further specifications about how the transformer is designed can be obtained in appendix A.

The load consist of 4 resistors - two of 15 kΩ and two of 10 kΩ (11 W each) - adding up to a total 50 kΩ. The size of the load resistance is chosen to maximize the power transfer (Figure 4.9). The behavior of the load at high frequencies is analyzed in appendix B.

An additional resistor of 1 kΩ is added to the system (appendix B). This is done to be able to do analyze the voltage before the impedance of the wheel in the circuit. If the voltage wave shape over the 1 kΩ differs from the one over the load, different currents are running through the resistors, and there is probably a leakage due to the big metal plate.

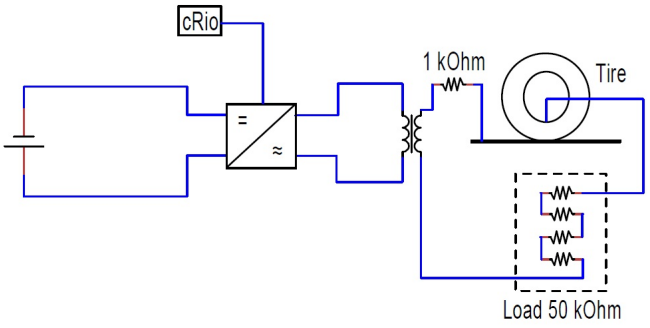

(a) Set-up circuit

(b) set-up

Figure 5.1: Set-up for practical experiment without resonant inductance

5.1.2 Method

The converter is set to provide a square wave voltage with a 9750 Hz frequency[6]. Measurements are done over the primary voltage and current of the transformer, the voltage over the small resistance and over one of the 10 kΩ resistors in the load. The measurements are made with a Tektronix TPS 2024 Oscilloscope and Tektronix P5200A Differential probes. The DC voltage is set to 30 V.

5.1.3 Results

Figure 5.2a and Figure 5.2b are showing the primary voltage and current respectively, when the DC voltage is set to 30 volts. The primary voltage is a square wave with a small over shoot at the beginning of each switch. The amplitude after the over shoot is close to the value of the DC link, which is expected as the only drop of voltage before the primary side of the transformer is over the transistors and the diodes in the converter.

The wave shape of the primary current can be explained by the load on the secondary side, the capacitive element of the transformer and the leakage inductance in the transformer: The big current transient in the beginning of each switch is due to the capacitive elements, which works almost like short circuits when the switch

[6]The reason for that the frequency is 9750 Hz is that a suitable LabView code already was available to achieve this, and that programming in LabView lies outside of the scope of this thesis.

in the voltage is fast. The oscillation in the signal implies that a inductance - due to that the magnetic linkage of the primary and secondary winding is not perfect (coupling factor is equal to 0.9988, read appendix A) - is present.

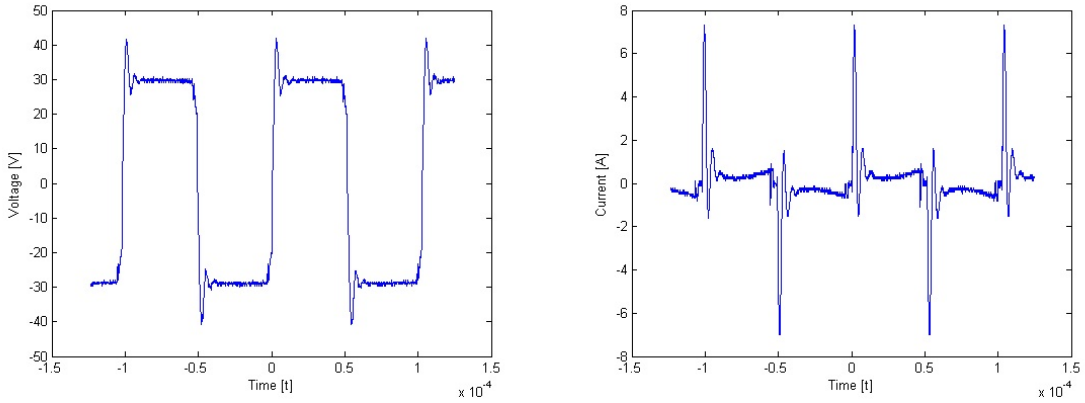

(a) Primary voltage (b) Primary current

Figure 5.2: Practical expreiments without resonance inductance: Primary voltage and current

Figure 5.3a and Figure 5.3b are showing the voltage over the 1 kΩ and the 10 kΩ of the load divided by 0.2 (assuming that the voltage is dividing linearly over the resistive elements), respectively. As can be seen the voltage shapes are quite different even if they theoreticaly should be the same (the same current should flow through the entire circuit). Even though there is a small capacitive element in the load (read Appendix B), the parts that contributes mostly to difference in wave shapes is probably the leakage capacitance that the big metal plate give rise to. It should be emphasized though that no measurement has been done to confirm this, and therefore it is only speculations.

The oscillation in the signals is once again due to differences between the ideal och the real transformer. Notice the similarities between the primary current (Figure 5.2b) and the voltage - hence the current - over the 1 kΩ resistance (Figure 5.3a). This suggests that there is not much leakage happening in between these elements.

Figure 5.4 is showing the load power based on the voltage over the 10 kΩ of the load. The power is derived using equation 5.1, where $V_{load} = V_{10k\Omega}/0.2$, assuming that the voltage is distributed linearly over the resistances in the load.

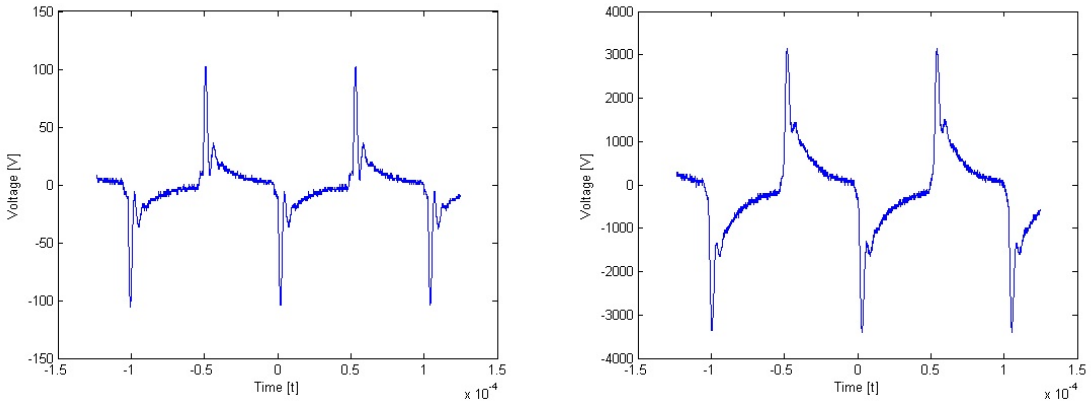

(a) Voltage over the 1 kΩ (b) Voltage over the load

Figure 5.3: Practical experiments without resonance inductance: Voltage over the 1 KΩ resistor and over the load

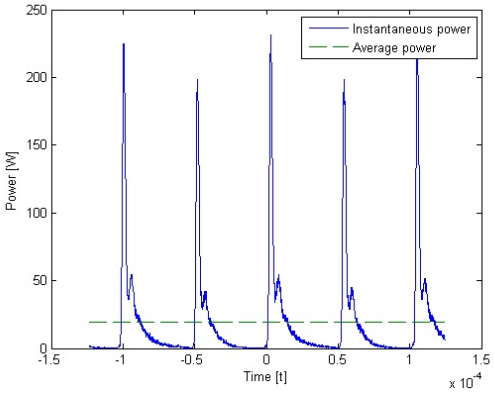

Figure 5.4: Practical experiment without resonance inductance: Load power

$$P_{load} = \frac{V_{load}^2}{R_{load}} \tag{5.1}$$

5.1.4 Comparison with LTspice

The goal of the LTspice simulation is to give results which are as close to the practical experiments as possible. The purpose of this is to have an idea of which imperfections that might be present in the components that are present when doing the practical experiments.

The LTspice model that is used in the simulations can be seen in Figure 5.5.

All the lumped parameters that are added which are not present in the ideal circuit are there to take account for imperfections in the components that are used in the practical experiments. Explanation for the parameters added to the transformer and the resistors can be read in Appendix A and Appendix B, respectively. The capacitance that is added in between the 1009 Ω and the 4020 Ω resistors are there to represent the capacitive leakage that the big metal plate give rise to. This value is obtained by comparing the the results from the practical experiments with the simulations.

The system is lacking a model of the inverter that is providing the practical experiments with a square wave voltage. Instead, an ideal voltage source is added that produces a square wave with the same rise and fall time as the inverter in the practical experiments provide. To have a more accurate result of the LTspice simulation, an inverter model should be implemented with the same characteristics as the one used in the practical experiments (this would affect both the wave shape of the source voltage, and the parasitic charactaristics - hence the efficiency - of the system).

The coupling factor of the transformer is first set to 0.9988, according to Appendix A. It becomes clear though, that when using a different value - 0.9943 - the simulation results become more similar to the results from the practical experiments. Simulation results using both of the values for the coupling factor is therefore presented.

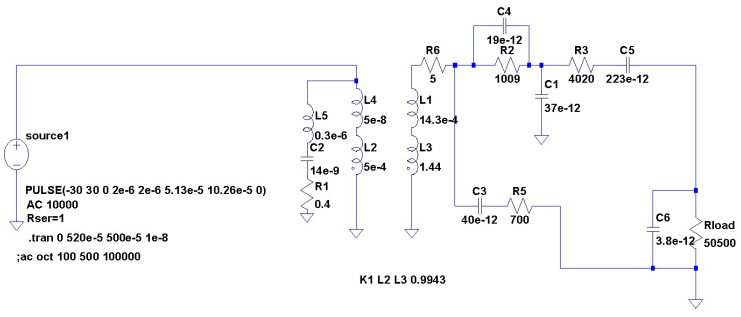

Figure 5.5: LTspice model over the system without resonant inductor

5.1.4.1 Results

A comparison between the simulations that are made in the LTspice software and the practical results that were obtained in the practical experiments are shown in Figure 5.13 and in Figure 5.14

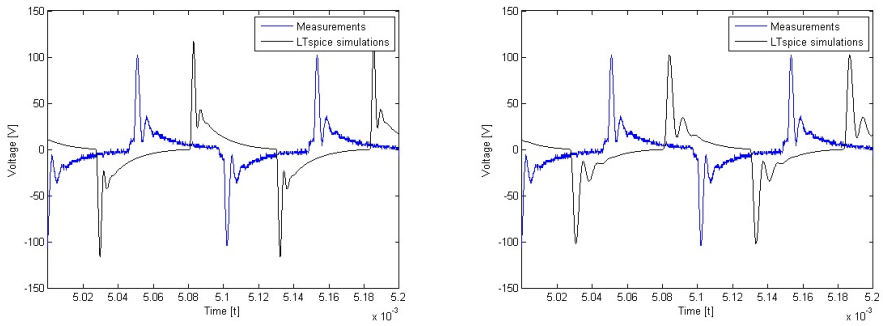

(a) Coupling factor: 0.9988 (b) Coupling factor: 0.9943

Figure 5.6: LTspice simulations without resonance inductance: 1 kΩ voltage, the curves are seperated time wise to be easier to analyze

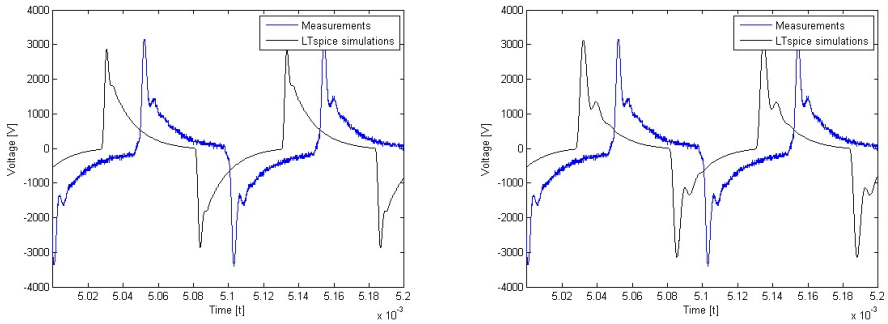

(a) Coupling factor: 0.9988 (b) Coupling factor: 0.9943

Figure 5.7: LTspice simulations without resonance inductance: load voltage, the curves are seperated time wise to be easier to analyze

5.2 With resonance

The second experiment introduces a resonance filter to the system.

5.2.1 The setup

The setup for the experiment with a resonant inductance is illustrated in Figure 5.8a and can be seen in Figure 5.8b. As can be seen, the set-up is the same as in the previous experiment, with the exception that an inductor is introduced in between the tire and the load.

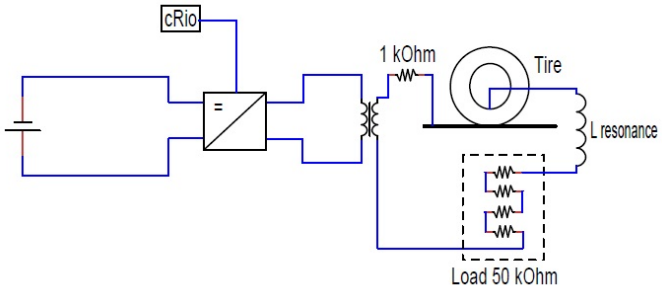

(a) Set-up circuit

(b) set-up

Figure 5.8: Set-up for practical experiment with resonant inductance

5.2.2 Method

The way that the right value for the inductance is found and how the inductor is made can be found in appendix C. To find the precise resonance though, the value of the inductance is manipulated manually by creating an air gap in the core while conducting the experiment. By checking how much current that is provided by the DC source, the value of the inductance is determined by investigating when most current is provided. When the right inductance value is found the experiments are conducted in the same way as in the preceding chapter.

5.2.3 Results

Figure 5.9a and Figure 5.9b are showing the primary voltage and current respectively. As can be seen, the voltage is very similar to the experiments without the resonant inductance, while the current almost have a sinusoidal wave shape with a big peak in the beginning of each half period. The sinusoidal wave shape can be explained by the resonant filter: The inductance is tuned in so there is (theoreticaly) no imaginary impedance for the fundamental frequency of the square

wave (9750 Hz). For the higher harmonics though, the inductance will result in a big impedance as the impedance value is linearly dependent off the frequency. The big peak is due to the parasitic parallel capacitance that is present in the resonant inductance. Since the impedance of the capacitance is inversely dependent on the frequency, the impedance will be very small for the higher harmonics in the square wave.

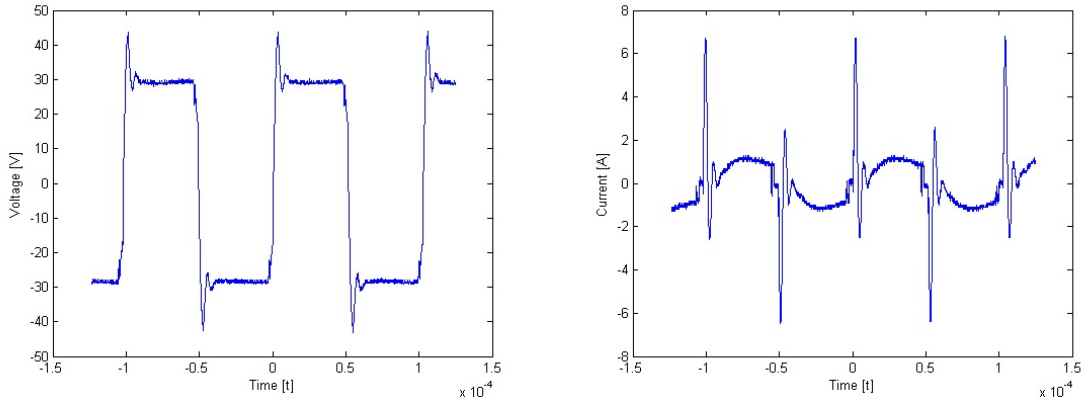

(a) Primary voltage (b) Primary current

Figure 5.9: Practical expreiments with resonance inductance: Primary voltage and current

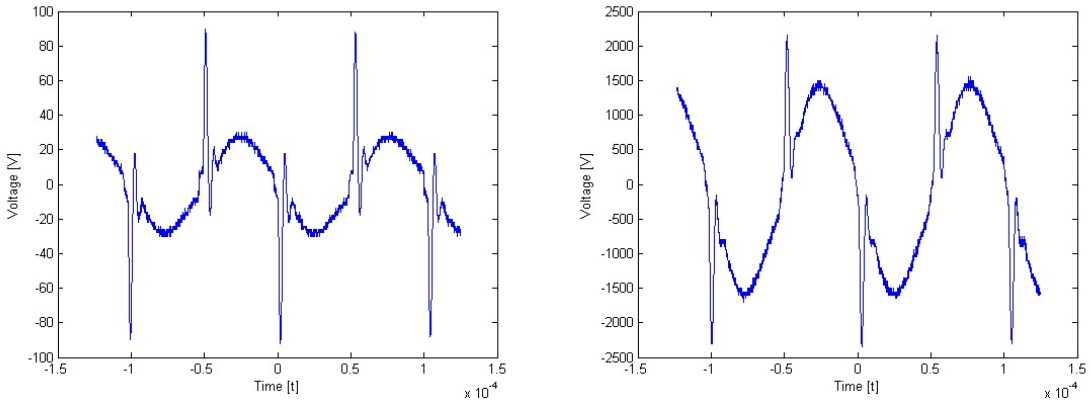

(a) Voltage over the 1 kΩ resistor (b) Voltage over the load

Figure 5.10: Practical expreiments with resonance inductance: Voltage over the 1 KΩ resistor and over the load

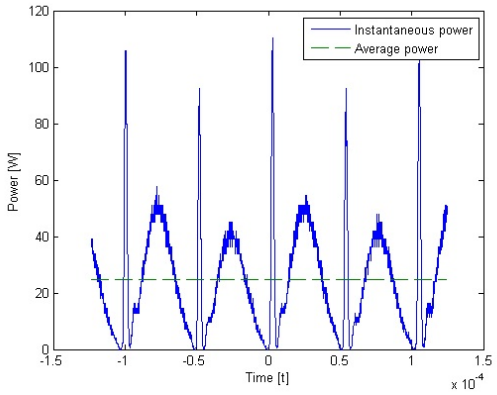

Figure 5.11: Practical expreiments with resonance inductance: Load power

5.2.4 Comparison with LTspice model

The LTspice model that is used to simulate the experiments with a resonance inductance can be seen in Figure **??**. The resonance inductance that is introduced (L6 in Figure **??**) is based on the measurements from Appendix C. It is important to emphasize that since the inductance is tuned in manually after the impedance measurements is made on it, the model is not a very good representation of the inductance that is used in the final experiments.

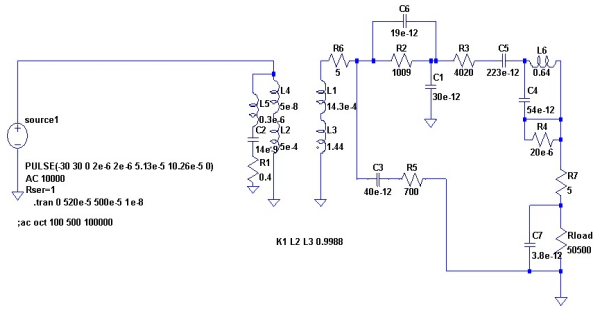

Figure 5.12: LTspice model over the system with resonant inductor

5.2.4.1 Results

A comparison between the simulations that are made in the LTspice software and the practical results that were obtained in the practical experiments are shown in Figure 5.13 and in Figure 5.14. The simulation results are not as close to the

practical results as in the case when no resonance is present. This implies that the model of the resonant inductor is not very accurate. Another interesting notion to be made is that - in contrast to simulation without resonant inductor - it is not clear if its the simulation with the coupling factor of 0.9943, or the coupling factor of 0.9988, that is closest to the practical experiments. This stresses the fact that that the analytical models that are constructed to mimic the practical experiments are only models and not reality, and that it is hard to know exactly which parameters that affects the system in what way.

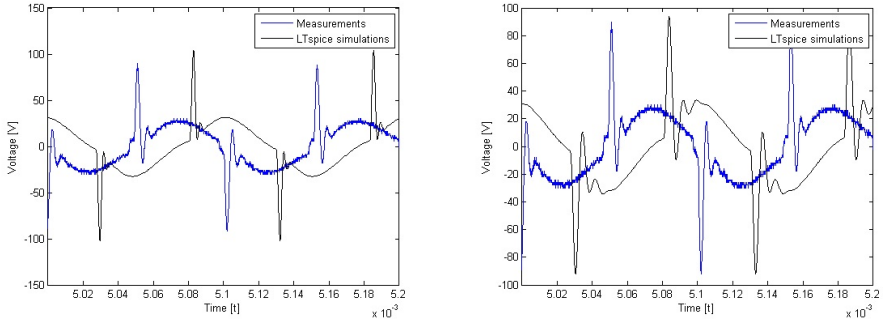

(a) Coupling factor: 0.9988 (b) Coupling factor: 0.9943

Figure 5.13: LTspice simulations with reonance inductance: 1 kΩ voltage, the curves are seperated time wise to be easier to analyze

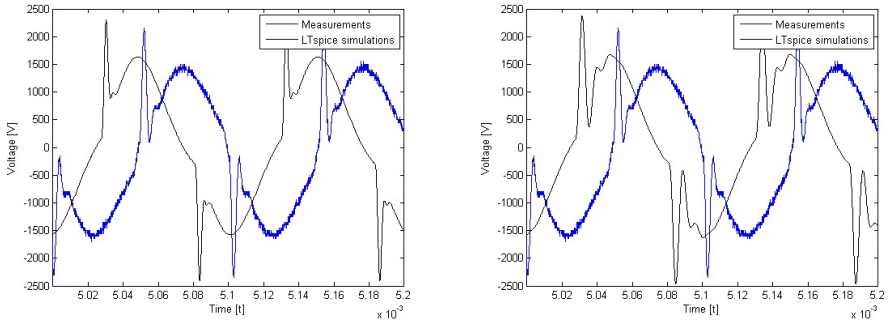

(a) Coupling factor: 0.9988 (b) Coupling factor: 0.9943

Figure 5.14: LTspice simulations with reonance inductance: load voltage, the curves are seperated time wise to be easier to analyze

5.3 Numerical results

The numerical results for the power transfer and the efficiency for the analytical model, the practical experiments and the LTspice simulations can be seen in Table 5.1.

Comparisons			
	Analytical model	Practical experiments	LTspice simulation
Without resonance inductor,			
Power transfer	21 [W]	19.5 [W]	19.6 [W]
Efficiency	89 %	81 %	81 %
With resonance inductor,			
Power transfer	34 [W]	24.6 [W]	25.2 [W]
Efficiency	89 %	76 %	81 %

Table 5.1: Comparing numerical results from the analytic models, the practical models and LTspice simulations

As expected, the LTspice model which takes imperfections in the elements used in the practical experiments into account is much closer to the practical experiments that the analytical model, which assumes a more simplified model (watch preceding chapter). Worth to notice is the difference between the LTspice model and the practical experiments when a resonant inductor is introduced. This is probably mainly due to that the model of the inductance is inaccurate. As mentioned before the impedance value was tuned in when the experiments was made, but the impedance measurements were made before the tuning, and the characteristics of the impedance were therefor not properly measured. A longer explanation is given in Appendix B.

Another point to be made is that the value that is used to calculate the efficiency of the power transfer in the practical experiments is the power that is coming out from the DC-source that provides the inverter with voltage. This is calculated by multiplying the voltage and the current, which is displayed on the DC-source. The problem is that the values that are displayed are rounded to only one decimal, which give possibilities for pretty high errors. For example, the voltage and current that was displayed for the experiment when a resonant inductor was 30 V and 1.1 A. But say for example that the values actually were 29.5 V and 1.05

A. This would mean that the efficiency actually would be 81 % which would be consistent with the LTspice simulation.

6. DISCUSSION

The results in the preceding chapters shows clearly that with the conditions that the practical experiments in this work are conducted, it is not possible to transfer enough energy for the technique to be of interest for a real life implementation. This chapter is focusing on discussing the parameters that can enhance the possibilities to transfer power through the tire. First, a discussion regarding the impedance features of the tire is held. Secondly, the impact of the frequency and amplitude of the source voltage is analyzed. Finally, a conclusion is made and pointers for an eventual proceeding with this topic is presented.

6.1 The impedance

The main factor for whether this technique will be useful or not is the characteristics of the impedance coupling between the plate and steel cord. Assuming that a resonant inductance can be implemented to compensate for the capacitance, the real pressing issue is the size of the equivalent series resistance that exists in the impedance coupling. This value is - as mentioned in Chapter 3 - dependent first and foremost on the polarization losses, which means the relative loss factor for the dielectric. [4] shows that adding carbon black - which is used as filler in the rubber compound of the tire - to rubber is increasing the loss factor considerably. Questions to ask is therefor, is there any alternatives to carbon black as filler? Is it possible to decrease the loss angle by manipulating the rubber compound?

The most frequently used filler, except for carbon black, is silica. [12] suggests that adding silica to styrene butadiene rubber actually decreases the loss constant where the carbon black increases it. This is by no means to be taken as that a tire with silica filler must be a better solution that a tire with carbon black filler - the dielectric constant goes down with the amount of silica in the rubber as well - but at least it is showing that it is not impossible to modify the dielectric properties of a tire.

Figure 6.1 is showing the power transfer to a load resistance of 100 Ω as a

function of the loss factor. This supposes that the series resistance only is dependent on the polarization losses, which is not true (3.2), and it also supposes that the dielectric constant is constant. The voltage is the same as is used in the previous simulations and the practical experiments, the dielectric constant is set to be ϵ=15 and the capacitance is set to be 200 pF.

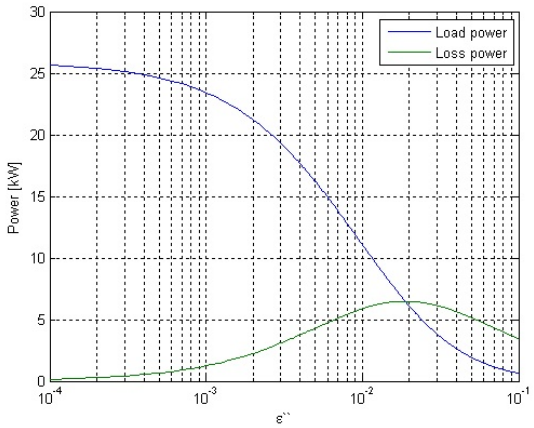

Figure 6.1: Power transfer as a function of Loss Factor

Even though the conditions are ideal in the graph, it still gives a hunch that with a small loss factor, large amounts of energy indeed can be transferred through the tire without big losses. If the technique that is presented in this thesis should be further investigated, this is where the main focus should lie.

6.2 The source voltage

Since the equivalent series resistance of the capacitive coupling is inversely dependent on the frequency, a higher frequency gives the possibility of a higher power transfer. Figure 6.2 shows the power transfer at a frequency of 100 kHz, using the analytical model with a sinusoidal voltage and a resonant inductor introduced.

As can be seen, even with a 10 times bigger frequency then the one used in the practical experiments, the power is still not close to sufficient to drive a electrical vehicle. As the resistance is inversely dependent of the frequency, the higher the frequency, the smaller change in the resistance value for a further increase in

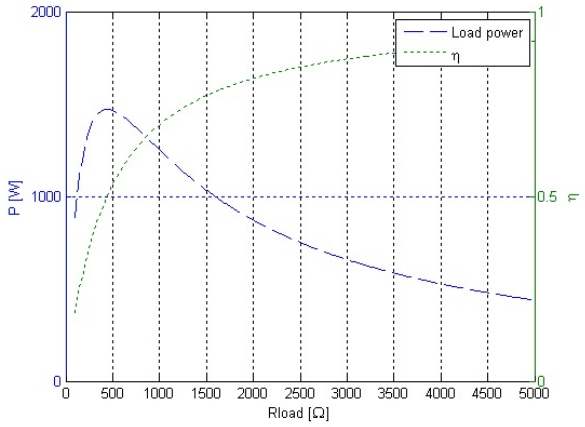

Figure 6.2: Power transfer with a source voltage frequency of 100 kHz

frequency. This implies that the frequency must be very high to achieve a desirable impedance characteristic of the tire. Further investigation about how high the frequency really can be needs to be done, but to achieve the power transfer that is necessary, one almost certainly have to change the dielectric characteristics of the rubber compound used in the tire.

As the power transfer has a quadratic relationship with the RMS value of the voltage, it is easy to estimate how a change would affect the power transfer. More research should be done regarding this to evaluate which voltage amplitude that is realistic to implement in the road.

6.3 Conclusion

This thesis evaluates the possibility to transfer electrical energy from a steel plate to the steel cord in a car tire with capacitive power transfer. The thesis shows that even though a small transfer is possible, the dielectric properties of the car tire used in the experiments makes it inappropriate for transfer of bigger amounts of energy. Assuming that one can find a tire with more favorable characteristics - or if the rubber compound can be modified so that the loss angle is decreased - continuous evaluation of this technique could indeed be interesting. If more work is to be done then, focus should lie on mixing with the dielectric characteristics of the tire.

LITERATURE CITED

[1] Energimyndigheten, *En ergilget 2011*, 2011

[2] Mats Alaküla, *Energy storage sytems*, 2011, obtained from homepage: http://www.iea.lth.se/hfs/Kurs% 20ht11/Lectures/EHS_L4_2011_hybrid.pdf

[3] Masahiro Hanazawa, Takashi Ohira, *Power Transfer for a Running Automobile*, Microwave Workshop Series on Innovative Wireless Power Transmission: Technologies, Systems, and Applications (IMWS), 2011 IEEE MTT-S International

[4] A. M. Bishai, A. M. Ghoneim, A. A. M. Ward & A. F. Younan,*Mechanical and dielectric properties of styrenebutadiene rubber polyester short-fiber composites: Part II. Composites loaded with high abrasion furnace carbon black*, 2010

[5] J. Huh, S. Lee, W. Lee, G. Cho, and C. Rim, Narrow-width inductive power transfer system for online electrical vehicles, IEEE Trans. Power Electron., vol. 26, no. 12, pp. 36663679, Dec. 2011 &

[6] G. A. J. Elliott, J. T. Boys, A. W. Green, and Magnetically coupled systems for power transfer to electric vehicles in Proc. Int. Conf. Power Electron. Drive Syst., Feb. 1995, p. 797801 &

[7] G. A. Covic, J. T. Boys, M. L. G. Kissin, and H. G. LU, A three-phase inductive power transfer system for roadway-powered vehicles, IEEE Trans. Ind. Electron., vol. 54, no. 6, pp. 33703378, Dec. 2007.&

[8] S. W. Lee, J. Huh, C. B. Park, N. S. Choi, G. H. Cho, and C. T. Rim, On-line electric vehicle using inductive power transfer system, IEEE Energy Convers. Congr. Expo., Sep. 2010, pp. 15981601. &

[9] Walter S. Zaengl, Prof. em. Dr.-Ing. Swiss Federal Institute of Technology (ETH), Zurich, Switzerland, *Dielectric spectroscopy in time and frequency domain for hv power equipment (transformers,cables etc.)*, 2001 &

[10] Allan R. Habley, *Electrical Engineering, Principles and Applications*, Fourth edition, 2008 &

[11] Loyd H. Dixon, Texas instruments, *Magnetics design for switching power supplies*, 2001.

[12] A. A. Ward, A. I. Khalf, Dokki Cairo, *Inuence of TESPT on the PhysicoMechanical and Dielectric Properties of Silica Filled SBR Composites*, 2009

APPENDIX A
The transformer

To be able to conduct the practical experiments in a satisfactory manner, a transformer is added to the system. A ratio of 1:50 is considered, giving the possibility to provide the experimental circuit with a 10 kV peak to peak voltage. An LTspice model is created to evaluate what influence the transformer has to the system. The LTspice model is also used to obtain suitable values for the primary and secondary inductance, with the goal to minimize the current spikes on the primary side. The number of turns that the primary and secondary winding should have is obtained by analytical calculations. When knowing the dimensions of the windings, the transformer is winded up manually. Since the transformer must handle a square wave voltage with a frequency of 10 kHz, a ferrite core is the best choice [11]. Laminated copper wire is used as conductors, twisting 5 wires for the primary and using one in the secondary winding. The winding impedances from the real transformer are measured, and an equivalent circuit is designed to take account for the imperfections in the inductances. The coupling factor is deduced using the measured impedance values, and is too taken account for.

A.1 Sizing

A good size for the primary and secondary inductor in the transformer is determined by empirical studies of a circuit in LTspice, and the primary and secondary are set to 0.5 mH and 1.25 H, respectively.

When the value of the impedances is known, the turns of the primary and secondary windings can be deduced, knowing the dimension and the dielectric properties of the core. The number of the turns of the winding (N) can be expressed by the inductance of the winding (L) and the reluctance of the core ($\mathcal{R}$) [10]:

$$N = \sqrt{\mathcal{R}L} \tag{A.1}$$

The reluctance is defined by the geometry and the permeability of the core.

In this case, the core is approximated to consist of three segments with different lengths and cross areas (Figure A.1). The expression for the reluctance becomes:

$$\mathcal{R} = \frac{1}{\mu_f}(\frac{l_1}{A_1} + \frac{l_2}{A_2} + \frac{l_3}{A_3}) \tag{A.2}$$

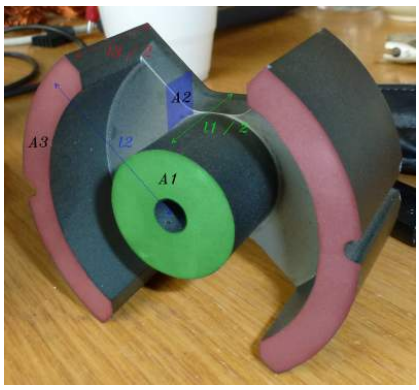

Figure A.1: Dimensions of transformer

Where μ_f is the permeability of ferrite and the A:s and l:s are the areas and lengths of the segments (Figure A.1). Using (A.1) the turns are calculated to 6.53 turns for the primary winding and 327 turns for the secondary. To get an even number of turns on the primary winding, it is rounded up to 7 turns, which results in 350 turns on the secondary. This results theoretically - in a primary inductance of 0.57 mH and a secondary inductance of 1.43 H. Measurements after the transformer is winded show a primary inductance of 0.5 and a secondary inductance of 1.43 H, which implies a transformer ration of 1:53.7.

A.2 Coupling factor

The coupling factor describes the magnetic connection between the primary and secondary inductor of the transformer, and is defined as in (A.3).

$$k = \frac{M}{\sqrt{L_p L_s}} \tag{A.3}$$

To be able to derive the coupling factor, an equation system that describes the voltage over the primary and secondary winding is set up.

$$V_p = L_p\frac{dI_p}{dt} + M\frac{dI_s}{dt} \quad (A.4)$$

$$V_s = M\frac{dI_p}{dt} + L_s\frac{dI_s}{dt} \quad (A.5)$$

Considering phasors, (A.4) and (A.5) can be rewritten as in (A.6) and (A.7).

$$V_p = j\omega(L_pI_p + MI_s) \quad (A.6)$$

$$V_s = j\omega(MI_p + L_sI_s) \quad (A.7)$$

If the secondary winding is short-circuited, (A.7) becomes:

$$0 = MI_p + L_sI_s \Rightarrow I_s = -I_p\frac{M}{L_s} \quad (A.8)$$

Substituting A.8 into A.6 an expression for the primary voltage as a function of the primary current can be reached:

$$V_p = j\omega I_p(L_p - \frac{M^2}{L_s}) \quad (A.9)$$

The primary inductance when the secondary winding is short-circuited then, can be defined as in (A.10).

$$L_{ps} = L_p - \frac{M^2}{L_s} \quad (A.10)$$

Considering A.3 and A.10, an expression for the coupling factor as a function of the primary inductance with the secondary open and the primary with the secondary closed can be reached:

$$k^2 = \frac{M^2}{L_pL_s} = \frac{L_s(L_p - L_{ps})}{L_pL_s} = 1 - \frac{L_{ps}}{L_p} \Rightarrow k = \sqrt{1 - \frac{L_{ps}}{L_p}} \quad (A.11)$$

Since the secondary inductance is much bigger than the primary, the measurements are done on the secondary in contrast to what the mathematical expressions above imply. This makes no difference since the same mathematical de-

duction could be done switching the primary for the secondary inductance. The relevant impedance values are measured with an Escort ELC-133A at 100 Hz to $L_s = 1500mH$ and $L_{ss} = 3.70mH$, and the coupling factor is calculated with(A.11) to $k = 0.9988$.

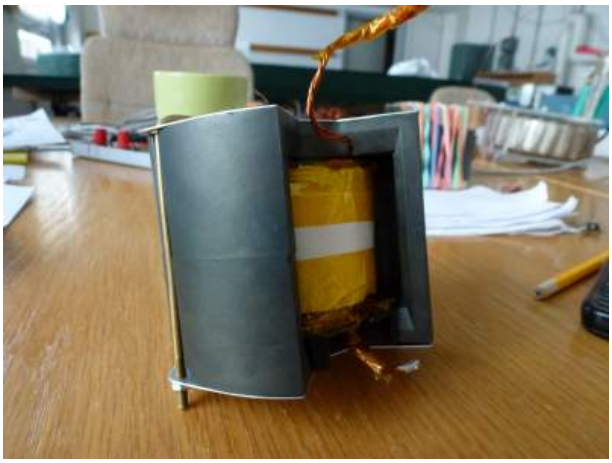

Figure A.2: Transformer

A.3 Analytical model of windings

To further get an idea of how the impedance features of the windings look like, the impedance of the windings are measured with a Hewlett packard 4194A impedance/gain-phase analyzer from 100 to 400000 Hz with the other winding short circuited. When one of the windings is short circuited, the impedance measurements on the other winding should theoretically be zero. This is not the case since there is leakage inductance, parallel capacitance and so on present. Of course, the lumped parameters are only a representation of the actual impedance, but by constructing an analytical model of the windings, the most obvious imperfections can be detected. Ideally, this should be done by doing a finite element simulation of all the elements - first and foremost the copper conductors and the core - and by the result build up an analytical model. Since that is way out of the scope of this thesis, an analytical model is derived by reasoning out how the model might look like based on the way the windings are wound, and then empirically try out which values that fit the measurements best.

A.3.1 Primary

The equivalent model of the primary winding can be seen in Figure A.3. Lleak represents the leakage inductance, which occurs since a small part of the magnetic flux passes through the air instead of sticking to the ferrite core. Lpar represents the inductance which occurs when the five copper wires that is used in the primary winding are twisted around each other. Cpar represents the capacitive coupling that occurs in between the copper wires. The resistance is added to represent the resistive part of the impedance in between the cooper wires.

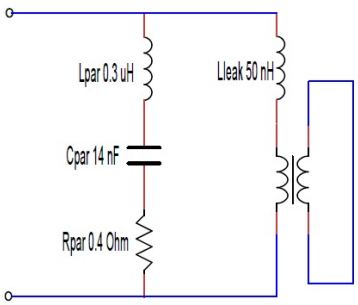

Figure A.3: Equivalent circuit of primary winding with the secondary short-circuited

The analytical expression for the equivalent circuit of the primary winding when the secondary is short-circuited becomes:

$$Z_{prim} = \frac{1}{\frac{1}{j\omega Lleak} + \frac{1}{j\omega Lpar + \frac{1}{j\omega Cpar} + Rpar}} \tag{A.12}$$

Figure A.4a and Figure A.4b are showing how consistent the equivalent model is with the impedance measurements. As can be seen, the model is not in any fashion perfect, but gives a hint of the biggest imperfections.

A.3.2 Secondary

The equivalent model of the secondary winding can be seen in figure A.4 Lleak represents the leakage inductance. No additional inductance is present since the copper conductors are not twisted together as in the case of the primary. Cpar

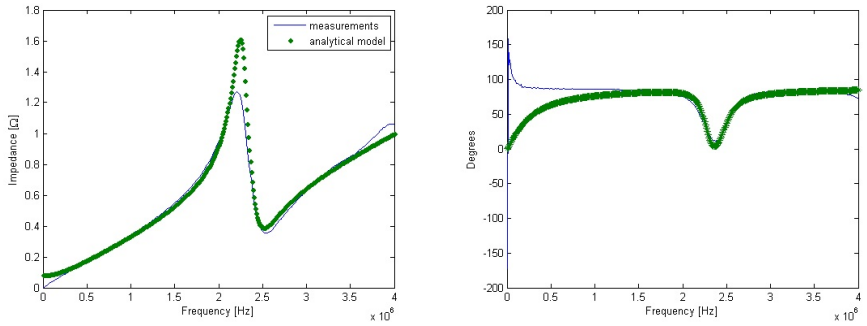

(a) Impedance amplitude, primary winding

(b) Impedance angle, primary winding

represents the capacitive coupling that occurs in between the copper wires and Rpar represents the parallel resistance. Rser represents the resistive losses in the copper.

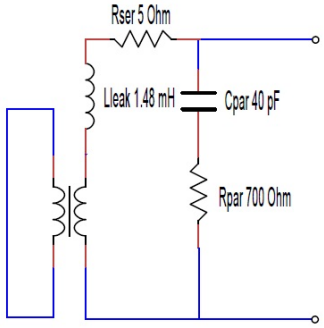

Figure A.4: Equivalent circuit of secondary winding with the primary short-circuited

The analytical expression for the equivalent circuit of the secondary winding when the primary is short-circuited becomes:

$$Z_{sek} = \frac{1}{\frac{1}{j\omega L_{leak}+R_{ser}} + \frac{1}{\frac{1}{j\omega C_{par}}+R_{par}}} \tag{A.13}$$

Figure A.5a and Figure A.5b are showing how consistent the equivalent model is with the impedance measurements.

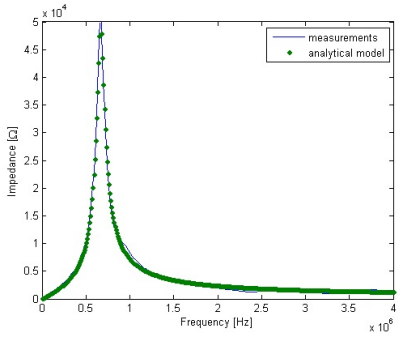

(a) Impedance amplitude, secondary winding

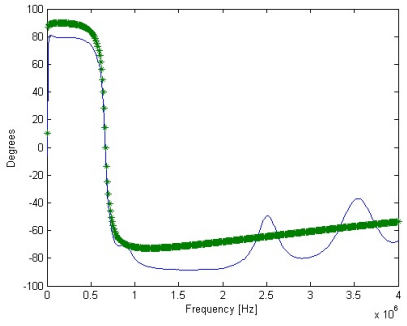

(b) Impedance angle, secondary winding

APPENDIX B
Resistive elements

B.1 The load

Figure B.1: The load

To be able to modulate the load - which consists of two 10 k$Omega$ and two 15 k$Omega$ resistors (11 W each) in series - in a good way, an equivalent circuit that takes the imperfections of the resistance into account can be seen in Figure B.2. The model is developed trying to emulate the characteristics of the load as accurately as possible. The analytical expression for the equivalent circuit can be seen in (C.1).

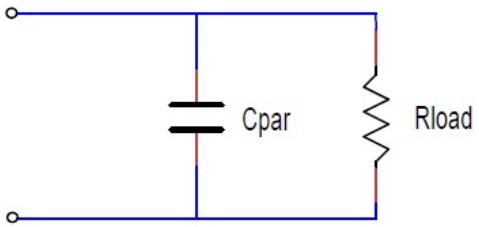

Figure B.2: Equivalent circuit of the load

$$Z_{load} = \frac{R}{1 + jR\omega C} \tag{B.1}$$

Figure B.3a and Figure B.3b are showing the measured impedance amplitude and angle as a function of frequency, together with (C.1) plotted as a function of the frequency. As can be seen, the impedance angle becomes negative at higher frequencies, which implies that a capacitive element is present. Table B.1 is showing the values of the elements in the equivalent circuit.

	R	C
Big load	50.5 [kΩ]	3.8 [pF]

Table B.1: Impedance values of equivalent circuit of the load

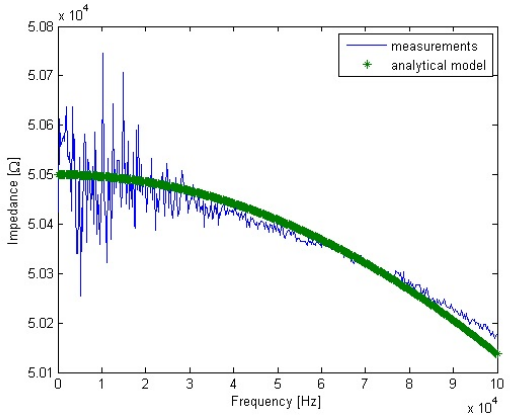

(a) Impedance amplitude, load

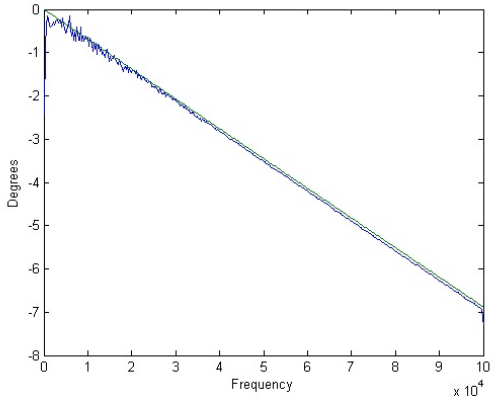

(b) Impedance angle, load

B.2 The 1 KΩ resistor

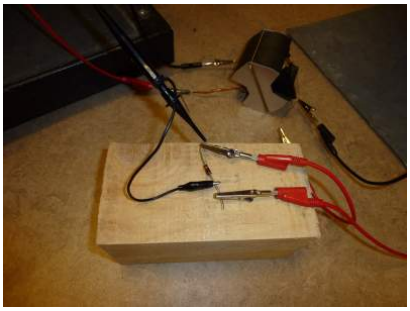

Figure B.3: The 1 kΩ resistor

The small load is examined in a similar fashion as the big load, using the same equivalent circuit - Figure B.2. The analytical expression for the equivalent circuit can be seen in (C.1).

Figure B.4a and Figure B.4b are showing the measured Impedance amplitude and angle as a function of frequency, together with (C.1) plotted as a function of the frequency. As can be seen, the impedance angle becomes negative at higher frequencies, which implies that a capacitive element is present. Table B.2 is showing the values of the elements in the equivalent circuit.

	R	C
Small load	1009 [Ω]	19.5 [pF]

Table B.2: Impedance values of equivalent circuit, 1 kΩ resistor

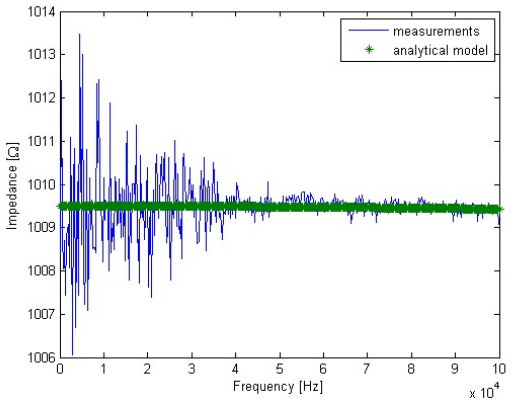

(a) Impedance amplitude, 1 kΩ resistor

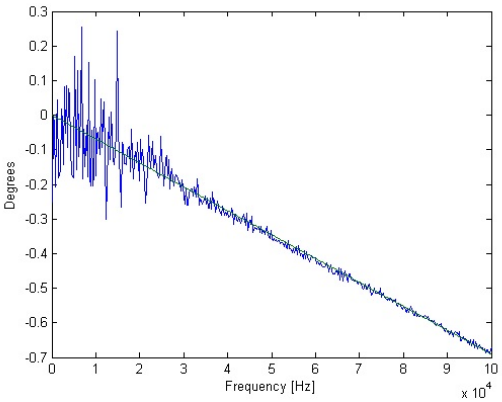

(b) Impedance angle, 1 kΩ resistor

APPENDIX C
Resonant inductance

The size of the inductance was deduced by knowing the value of the capacitance of the impedance coupling of the metal plate and the tire at 10 kHz, using (4.22). Since the permeability of the core of the inductor could not be found, the good inductance value was found by measuring the inductance after a number of turns was wound, and based on that measurement adding or reducing the number of turns till the right size was achieved. The inductor can be seen in figure C.1.

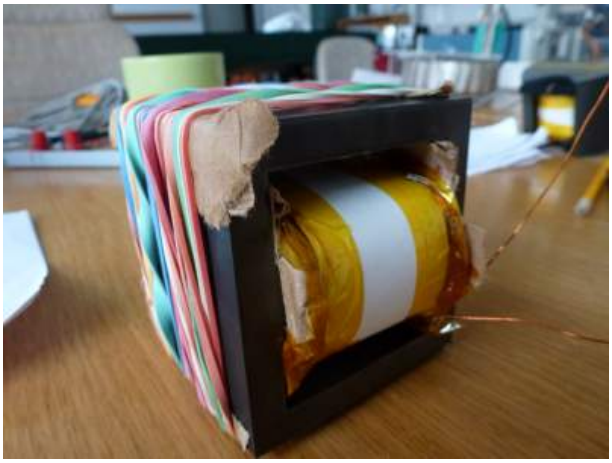

Figure C.1: The resonance inductance

An equivalent circuit for the inductance was found using the same method as for the primary and secondary of the transformer. It should be emphasized here that this measurements was made before the fine tuning of the inductance was done when conducting the experiments. That means that the characteristics that is shown in Figure C.3a and Figure C.3b are not the exact same as for the inductance used in the experiments, but close. The analysis is still helpful since it shows that a big capacitive element is present in the inductor, which of course affects the results of the experiments.

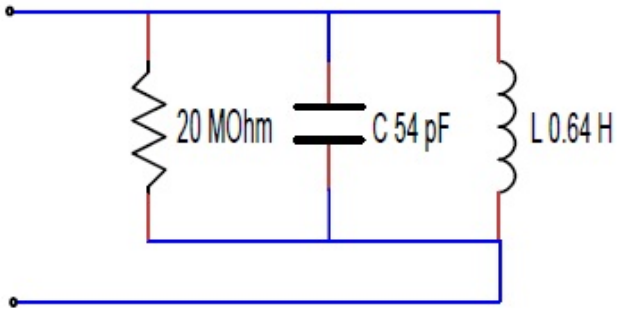

Figure C.2: Equivalent circuit of resonance inductance

The analytical expression for the equivalent circuit of the inductor becomes:

$$L_{res} = \frac{1}{\frac{1}{R} + \frac{1}{j\omega L} + j\omega C} \tag{C.1}$$

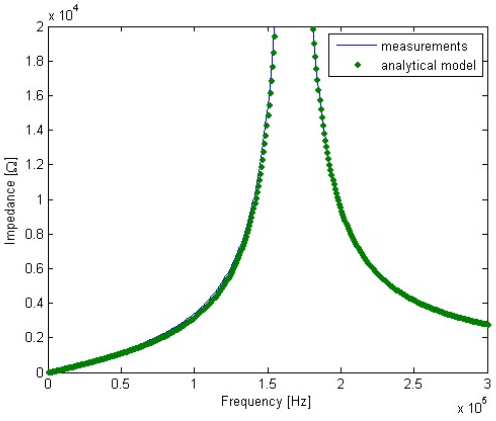

(a) Impedance amplitude, resonance inductance

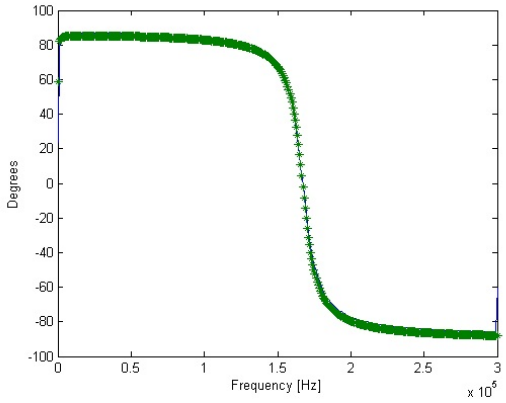

(b) Impedance angle, resonance inductance